Highlights

- Lake-level reconstructions can be used to reconstruct hydroclimatic changes
- Northern (Southern) Europe becomes more arid (humid) during abrupt cooling events
- European hydroclimatic changes were more dynamic than changes in temperature
- Hydroclimatic changes were not concurrent with $\delta_{18}O$ in the Greenland ice cores

# Hydroclimatic changes in the British Isles through the Last-Glacial-Interglacial Transition: multiproxy reconstructions from the Vale of Pickering, NE England.

Paul C. Lincoln[a, b], Ian P. Matthews[a], Adrian P. Palmer[a], Simon P.E. Blockley[a], Richard A. Staff[c], Ian Candy[a]

[a] Centre for Quaternary Research, Department of Geography, Royal Holloway, University of London, Egham, UK.

[b] Present address: School of Archaeology, Geography and Environmental Science, University of Reading, Earley, UK

[c] Scottish Universities Environmental Research Centre, University of Glasgow, East Kilbride, UK

## Abstract

European paleoenvironmental records through the Last Glacial-Interglacial Transition (LGIT; *ca* 16-8 cal ka BP) record a series of climatic events occurring over decadal to multi-centennial timescales. Changes in components of the climatic system other than temperature (e.g. hydrology) through the LGIT are relatively poorly understood however, and further records of hydroclimatic changes are required in order to develop a more complete understanding on the phasing of environmental and anthropogenic responses in Europe to abrupt climate change. Here, we present a multiproxy palaeoenvironmental record (macroscale and microscale sedimentology, macrofossils, and carbonate stable isotopes) from a palaeolake sequence in the Vale of Pickering (VoP), NE England, which enables the reconstruction of hydroclimatic changes constrained by a radiocarbon-based chronology. Relative lake-level changes in the VoP occurred in close association (although not necessarily in phase) to threshold shifts across abrupt climate change transitions, most notably lowering during cooling intervals of the LGIT (~GI-1d, ~GI-1b, and ~GS-1). This reflects more arid hydroclimates associated with these cooling episodes in the British Isles. Comparisons to hydrological records elsewhere in Europe show a latitudinal bifurcation, with Northern Europe (50-60°N) becoming more arid (humid), and Southern Europe (40-50°N) becoming more humid (arid) in response to these cooling (warming) intervals. We attribute these bifurcating signals to the relative positions of the Atlantic storm tracks, sea-ice margin, and North Atlantic Polar Front (NAPF) during the climatic events of the LGIT.

## 1. Introduction

The Last Glacial-Interglacial Transition (LGIT; *ca* 16-8 cal ka BP) is the most recent period of large-scale reorganisations in ocean-atmospheric circulation. This reorganisation had profound and far reaching impacts on global climate (Heiri et al*.,* 2014; Rahmstorf et al*.,* 2015). The stratotype for the LGIT in the circum-North Atlantic region is the Greenland oxygen isotope ($\delta^{18}O$) event stratigraphy, where a series of abrupt and short-lived (millennial to centennial scale) climatic events (GI-1d, GI-1c2, GI-1b, GS-1, 11.4 ka event) are detected (Rasmussen et al*.,* 2014). The cause of these events are debated, but likely reflect fluctuations in the strength and position of the Atlantic Meridional Overturning Circulation (AMOC) in the North Atlantic Ocean, driven by freshwater forcing from the deglaciation of Northern Hemisphere ice sheets (Broecker and Denton, 1989; Clark et al., 2002; Marshall et al., 2007). The LGIT provides a key interval for examining the terrestrial and hydrological responses to intervals of abrupt climatic change in Europe (e.g. Vellinga and Wood, 2002; Heiri et al., 2014).

The general millennial-scale patterns of climate change during the LGIT are well established in the Greenland ice cores and broadly correspond with palaeo-records from the mid-latitudes of the North Atlantic seaboard. However, spatial differences in the magnitude and synchroneity of shorter-lived climatic oscillations and their transitions remain largely untested assumptions (e.g. Lowe et al., 1995). Quantified palaeorecords of climate available for this period tend to focus on proxies of past temperature changes (Atkinson et al*.,* 1987; Yu and Eicher, 1998; von Grafenstein et al., 1999; Brooks and Birks, 2000; Marshall et al., 2002; Brooks et al., 2012) and have sought to identify the degree of coherence with the Greenland ice-core records. However, recent studies have highlighted that other climatic factors, particularly hydrological variability, are also important during abrupt climatic events recorded in the mid latitudes (e.g. Renssen et al., 2018). These hydrological changes are thought to lead to substantial impacts on terrestrial landsystems e.g. glacier ice growth and decay (Boston et al., 2015; Mangerud et al., 2016; Chandler et al., 2019; Lowe et al., 2019), fluvial activity (Vandenberghe, 2008), vegetation cover (Birks and Birks, 2014) and phases of human migration and subsistence (Blockley et al., 2018).

To date, the limited number of studies have highlighted that significant spatial and chronological heterogeneity exists, specifically: (1) the transitions in to and out of the major intervals of the LGIT (i.e. the start of GI-1, GS-1, the Holocene) may be regionally diachronous (Buizert et al., 2014; Rach et al., 2014; Muschitiello et al., 2015); (2) there are centennial-scale hydroclimatic events which affect Europe and have no correlative in the Greenland ice-core $\delta^{18}O$ stratigraphy (Bakke et al., 2009; Lane et al., 2013; Guillevic et al., 2014; Blockley et al. 2018); and (3) the hydrological impact of these climatic events is spatially heterogeneous (Magny et al., 2003; Moreno et al., 2014; Renssen et al., 2018). However, testing these inferences is limited by the reliance on small numbers of available archives, insufficient chronological control to understand phasing, sites only containing partial records of the LGIT period and low inter-site sampling density within regions and/or between regions. These issues also inhibit our understanding of any latitudinal and longitudinal gradients that might exist, particularly with relation to hydroclimate, with only Hässeldala Port in Southern Sweden providing temporally well constrained hydrological data north of mainland Europe through part of the LGIT (i.e. between *ca* 13.5 – 11 ka BP; Muschitiello et al., 2015; Wohlfarth et al., 2017).

Here, we address the lack of combined quantified temperature and hydroclimatic data available from this part of NW Europe by presenting a new multiproxy palaeo-record of temperature and hydrological change from a palaeolake sequence in the Vale of Pickering (VoP) in NE England (54.2 ºN, 0.7 ºW; Figure 1). Specifically, we generate reconstructed temperature and hydrological variability from isotopic, sedimentological and palaeoecological proxies for the entire LGIT period constrained by a robust radiocarbon-based age model. The results suggest that hydrology is profoundly influenced by abrupt climatic oscillations and that strong heterogeneous responses are identifiable across latitudinal gradients.

## 2. Site context

The VoP is a low-lying valley in NE England situated adjacent to the North Sea coast (Figure 1). Between *ca* 25 and 17 ka BP the North Sea Ice Lobe (NSIL) advanced into the eastern 12 km of the VoP, forming a proglacial lake (Lake Pickering) and depositing a complex series of glacial, glaciolacustrine (Kendall, 1902; Evans et al., 2017), and glaciofluvial deposits (Palmer et al., 2015; Lincoln et al., 2017). After ice recession from the VoP, small palaeobasins formed within topographic depressions in the glacigenic sediments, which were subsequently infilled with lacustrine and alluvial deposits through the LGIT (Lincoln et al., 2017). The largest of these palaeobasins, Palaeolake Flixton (*ca* 4.2 km$^2$), has been extensively investigated via sedimentological (Palmer et al., 2015), palaeoenvironmental (Day, 1996; Candy et al., 2015; Blockley et al., 2018) and archaeological (Mellars and Dark, 1998; Milner et al., 2018) surveys. These studies have shown that palaeolake records in the eastern VoP have significant potential to reconstruct palaeoenvironmental regimes, but that the sediments from Palaeolake Flixton contain insufficient terrestrial plant macrofossil remains for the generation of robust radiocarbon-based age models prior to the Holocene (Day, 1996; Blockley et al., 2018).

The palaeolakes in the VoP provide significant potential for the reconstruction of hydrological regimes as they lie within porous, groundwater-fed glaciofluvial strata. The groundwater in the VoP is dominated by meteoric recharge (Bearcock et al., 2016) and has a low residence time (Brown et al., 2011), meaning it responds rapidly to changes in regional precipitation and is therefore a valuable proxy for changing hydrological conditions in the valley (section 3.3). The sedimentary sequences contained within Palaeolake Flixton contain evidence for substantial changes in lake-level that have been tentatively linked to broader hydrological shifts (Palmer et al., 2015). However, these shifts have yet to be independently corroborated or chronologically constrained (see above), meaning their link to the hydrology of the eastern VoP, and regional climatic changes remain unresolved.

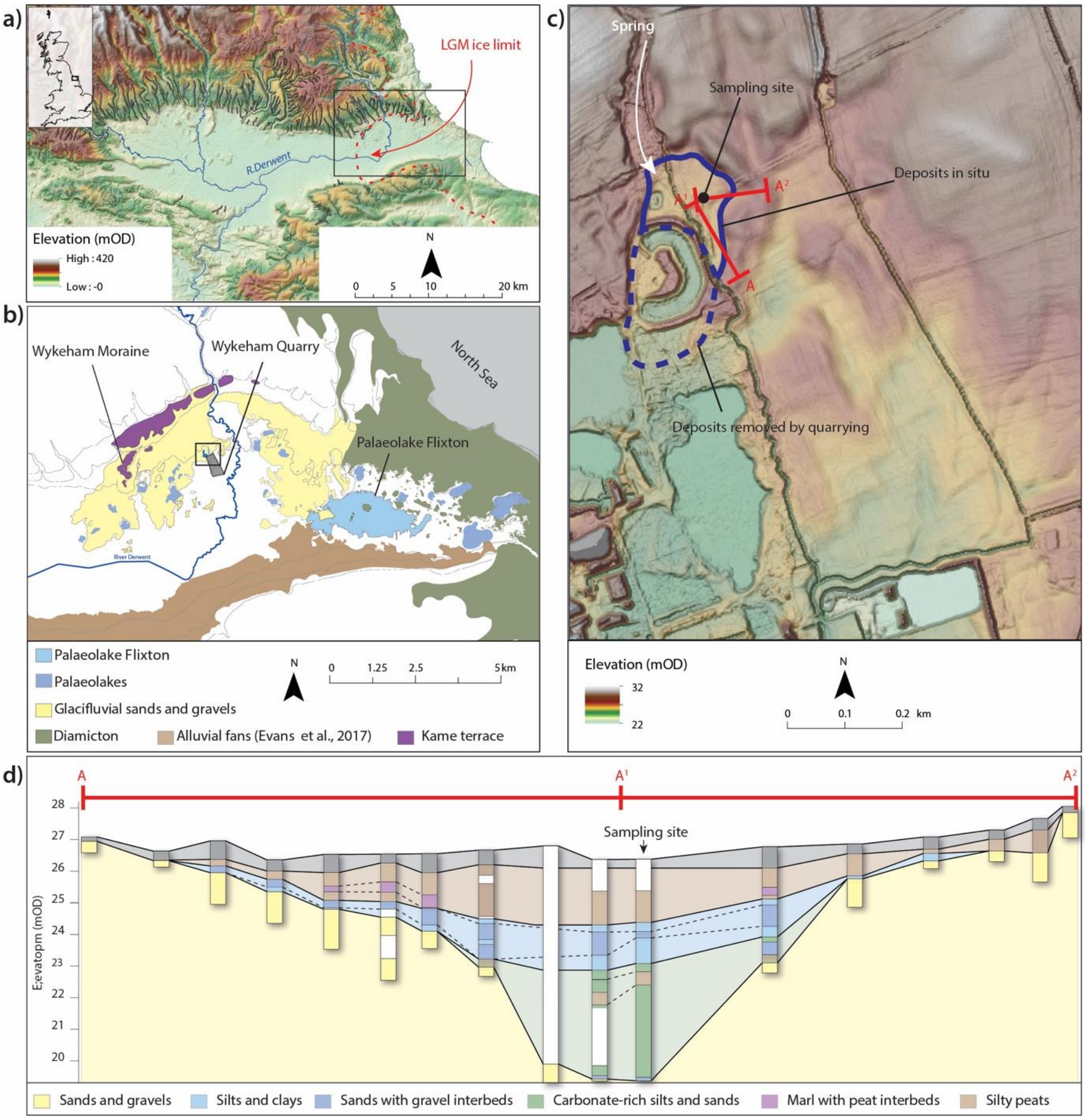


Figure 1. a) Digital Elevation Model (DEM) of the VoP with the LGM ice limit marked in red; b) map from Lincoln et al. (2017) showing the distribution of glacigenic sediments and palaeobasins in the eastern VoP, the location of Wykeham Quarry is in grey; c) LiDAR DEM of the study site, showing the extent of the palaeobasin and the sampling location of the sedimentary sequence; d) cross-section of the palaeolake, illustrating that the sedimentology and stratigraphy of the sampled sequence is representative of the broader palaeolake deposits.

Consequently, other palaeolakes in the eastern VoP were sought in the vicinity of Palaeolake Flixton, using desk-based GIS and depositional modelling around the Wykeham Quarry area to develop independent records of hydroclimatic change through the LGIT. A new kettlehole palaeolake, referred to as the Wykeham basin, was identified in glacifluvial outwash deposits ~ 4 km east of Palaeolake Flixton (Lincoln et al., 2017). The Wykeham basin is a small first order lake with a restricted catchment, a single spring-fed river input of less than 300 m length and direct coupling to the surrounding slopes (Figure 1b), meaning that the lake-level would have been sensitive to changes in the local groundwater. Therefore, the smaller (*ca* 0.03 $km^2$) and simpler characteristics of the Wykeham Basin mean that the deposits are potentially better suited to reconstruct and temporally constrain hydroclimatic changes in the valley than those in Palaeolake Flixton (Figure 1b-c).

## 3. Methodology

### 3.1. Sediment recovery and analysis

The extent, thickness, and sedimentology of the Wykeham basin infill was evaluated by exploratory augering with Eijkelkamp open gouge percussion coring, Russian coring, and deposit modelling of the area around Wykeham Quarry (Lincoln et al., 2017). This showed that the southwestern extent of the basin had been removed by quarrying, but the northern and eastern sections remain *in situ* (Figure 1; Batchelor, 2009; Lincoln et al., 2017). A further twenty-two overlapping, hand augered Russian and percussion augered stitz cores were obtained from five parallel boreholes spaced < 5 m apart in the deepest section of the basin (SE 98656 83093). A composite 6.80-m stratigraphy was constructed by correlating overlapping cores using key marker horizons and patterns in bulk sedimentology (Figure 2).

The calcium carbonate content of sediment samples was determined using a Bascomb calcimeter (Gale and Hoare, 1991). Repeat measurements were taken every 10 samples to check for measurement consistency. Carbonate content is expressed as the % dry weight of the sample. Organic content was determined via the loss-on-ignition (LOI) method following Dean (1974). The percentage of siliclastic content was calculated as 100 – (carbonate content + organic content) of each sample. Thin section analysis was used to describe and interpret sedimentological changes of carbonate fabrics through the core sequence, and to guide bulk sediment isotopic analysis. Thin section samples were prepared using the standard procedure of Palmer et al. (2008) and described following the terminology and protocol of Bullock et al. (1985). Full thin section descriptions and interpretations are presented in Appendix A.

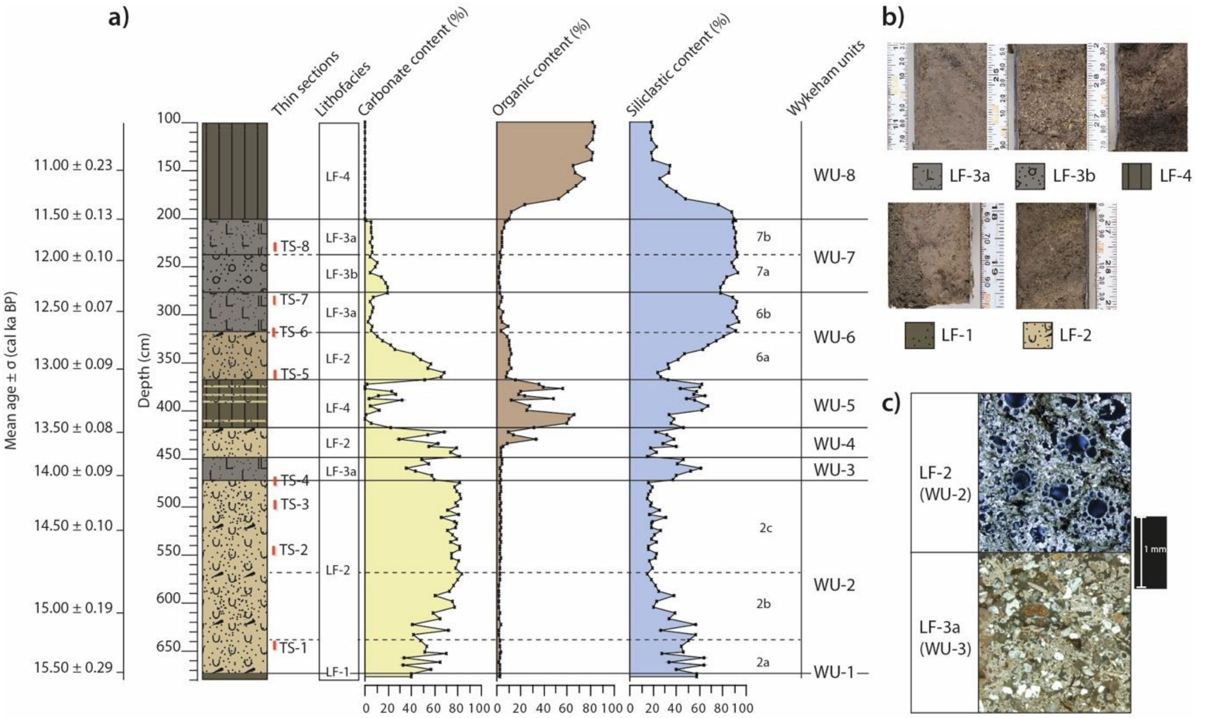


Figure 2. a) Summary of the sedimentology and stratigraphy of the Wykeham sequence with the lithofacies and Wykeham unit codes discussed in the text. Mean ages from the P_Sequence age-depth model (Figure 3) are included for reference. b) core images of the lithofacies coupled with the key for the stratigraphy used in a). c) Cross-polarised thin-section images from TS-2 in WU-2 & TS-4 in WU-3, illustrating the different sedimentological characteristics of the carbonates in the two lithofacies. LF-2 is comprised of high numbers of calcified charophyte thalli which form a significant proportion of the carbonate content whilst LF-3a consists of highly fragment charophyte remains interbedded with minerogenic material indicating a less stable depositional environment with carbonate content likely being reworked prior to final deposition (Appendix A).

Macrofossil analysis was undertaken on 2-cm-thick samples between 680 and 100 cm to identify key taxa to reconstruct the lake's evolution, and to provide material for radiocarbon dating (section 3.2). Sample volume was measured by the displacement of water in a measuring cylinder (Birks, 2002). Sediments were sieved over a 125 µm mesh, with sodium pyrophosphate ($Na_4P_2O_7$) added to the sediment when necessary to aid disaggregation. Macrofossils were identified and counted using a stereo light microscope at between x10 and x40 magnification using the reference collection at Royal Holloway, University of London, and identification guides (Berggren, 1964; Birks, 1980; van Geel et al., 1980; 1989; Watson, 1981; Smith and Smith, 2004; Cappers et al., 2006; Mauquoy and van Geel, 2007). Incomplete and/or very abundant remains such as mosses, leaf and wood fragments, and *Chara* thalli, were assigned a value on a 5-point, abundance scale (Birks and Matthewes, 1978; Birks, 2002; termed as AB), ranging from absent=0, present=1 (n=1-10), rare=10 (n=10-25), frequent=25 (n= 25-50), abundant=50 (n=50-100), very abundant= 100 (n=>100). Macrofossil counts are standardised to numbers per 50 $cm^3$ of sediment.

Bulk carbonate $\delta^{18}O$ and $\delta^{13}C$ analyses ($\delta^{18}O_c$ and $\delta^{13}C_c$ respectively) was conducted on samples between 674 and 339 cm, where micromorphological analysis showed that carbonate was derived almost entirely from micrite and microspar calcite crystals deposited either around charophyte thalli, or within a carbonate-rich matrix (section 4; Appendix A), which is consistent with authigenic carbonates precipitated within a lake body (e.g. Tye et al., 2016). No samples were taken from above 339 cm as the sedimentological and micromorphological data indicated that carbonate was present in very low abundances and was derived from detrital material including local limestone clasts. Contaminant carbonate fabrics (limestone clasts, charophyte thalli casts, ostracod carapaces and gastropod shells) were removed from the samples using fine forceps under a stereo light microscope, before being rinsed over 200 μm and 64 μm meshes to remove any remaining contaminant fabrics. To remove organic material from the samples, the <64 μm fraction was immersed in 10 % $H_2O_2$ until the reaction ceased (typically 1 to 3 days). Samples were then rinsed five times with deionised water and centrifugated to remove any residual $H_2O_2$, before being air-dried and powdered. Although there are concerns about whether the use of an aggressive oxidant may impact isotopic values, through our work in the VoP (Candy et al., 2015; 2017; Blockley et al., 2018) we have employed a range of methodological approaches for the preparation of isotope samples (sieved samples with no chemical treatment, drilled samples from impregnated sediment blocks and $H_2O_2$ pre-treatment). The results of these different methods have been entirely consistent and there is therefore no evidence that the use of 10 % $H_2O_2$ has a significant impact on the isotopic values of these samples. A Mettler Toledo XP6 microbalance was used to weigh samples to between 600-1200 μg and $\delta^{18}O_c$ and $\delta^{13}C_c$ values were determined using a VG PRISM series 2 mass spectrometer at Royal Holloway, with internal (RHBNC) and external (NBS19, LSVEC) standards run every 4 and 18 samples respectively. The isotope values were normalised to the V-PDB scale using the measured values from the standards and produced 1σ measurement uncertainties of ± 0.04 ‰ for $\delta^{18}O_c$ and ± 0.02 ‰ for $\delta^{13}C_c$.

### 3.2. **Radiocarbon-based chronology**

Accelerator mass spectrometry (AMS) derived radiocarbon ages were obtained from terrestrial plant macrofossil samples from the Wykeham sequence (Table 1). Sample preparation followed that for the macrofossil samples (section 3.1), with remains picked using fine metal forceps into glass vials, filled with 2 ml of 10 % HCl, topped up with deionised water, and refrigerated to prevent mould growth.

Radiocarbon activity of the samples was determined at the Oxford Radiocarbon Accelerator Unit (ORAU), at the University of Oxford, the Scottish Universities Environmental Research Centre (SUERC), and the University of California, Irvine (UCI) following standard acid-base-acid pre-treatment and analytical procedures (Brock et al., 2010).

Table 1. Radiocarbon dates from the Wykeham sequence used to construct the age-depth model shown in Figure 3. $\delta^{13}C$ ranges for the dates support that the carbon was derived from terrestrial sources and that their radiocarbon age ranges are therefore not affected by substantial reservoir ages (e.g. Lowe et al., 2019). Posterior outlier values from the applied General outlier model are also listed, demonstrating coherent age depth relationships for all but three of the dates (OxA-32441, OxA-32434, and SUERC-84464).

| Depth (cm) | Lab ID | Material | $\delta^{13}C$ (‰) | Radiocarbon date (BP) | Calibrated mean $\pm \sigma$ (cal a BP) | Outlier model posterior probability (%) |
|---|---|---|---|---|---|---|
| 200-198 | OxA-32343 | *Betula* undiff. leaf fragments | -29.5 | 9925 $\pm$ 50 | 11360 $\pm$ 100 | 4 |
| 234-231 | OxA-32397 | Twigs (undiff.) | -29.1 | 10205 $\pm$ 45 | 11910 $\pm$ 95 | 2 |
| 281-279 | SUERC-84465 | Twigs (undiff.) and *B.nana* leaf fragments. | -28.2 | 11036 $\pm$ 45 | 12901 $\pm$ 71 | 100 |
| 305-301 | SUERC-84464 | *Betula nana* and Asteraceae seeds, x2, *S.herbacea* leaf fragments and twigs undiff. | -27.6 | 10594 $\pm$ 43 | 12581 $\pm$ 61 | 1 |
| 313-308 | SUERC-84459 | *Salix herbacea,* and Ericaceae undiff. leaf fragments | -28.6 | 10693 $\pm$ 44 | 12653 $\pm$ 38 | 1 |
| 347-345 | OxA-32434 | *Carex* achenes and *Betula* undiff. seeds | -28.1 | 11520 $\pm$ 45 | 13363 $\pm$ 48 | 98 |
| 376-374 | OxA-32441 | Twigs (undiff.) | -28.6 | 11540 $\pm$ 50 | 13376 $\pm$ 51 | 74 |
| 379-377 | OxA-30541 | *Carex* seeds with perigynium | -27.1 | 11210 $\pm$ 140 | 13060 $\pm$ 147 | 3 |
| 400-398 | OxA-30030 | *Carex* seeds | -28.9 | 11475 $\pm$ 45 | 13327 $\pm$ 54 | 2 |
| 417-413 | OxA-32401 | Twigs (undiff.) | -27.9 | 11420 $\pm$ 50 | 13257 $\pm$ 61 | 28 |
| 446-444 | OxA-32436 | *Juniperus communis*. needles, leaf frags. (undiff.) | -26.5 | 11895 $\pm$ 50 | 13696 $\pm$ 73 | 2 |
| 480-478 | OxA-32437 | *B.nana* leaf frags and twigs (undiff.) | -27.2 | 12320 $\pm$ 55 | 14325 $\pm$ 161 | 3 |
| 481-480 | OxA-32435 | Twigs (undiff.) and *B.nana* leaves | -26.9 | 12340 $\pm$ 50 | 14359 $\pm$ 161 | 2 |
| 554-550 | SUERC-84458 | *Betula nana* leaves, fruits, budscales, catkin scales and undifferentiated twigs | -29.5 | 12603 $\pm$ 48 | 14955 $\pm$ 128 | 14 |
| 592-586 | SUERC-84457 | *Potentilla erecta, Saxifraga* undiff. seeds, *Betula* undiff. catkin scale and undiff. leaf fragments | -23.7 | 12560 $\pm$ 50 | 14871 $\pm$ 158 | 4 |
| 636-633 | SUERC-84456 | Twig, leaf fragments undiff., *Cerastium* sp. and *Taraxacum* seeds | -27.3 | 12509 $\pm$ 47 | 14747 $\pm$ 187 | 36 |
| 641-636 | UCIAMS-216468 | *Poaceae* seeds, *Taraxacum* seed and twigs undiff. | | 12500 $\pm$ 40 | 14729 $\pm$ 181 | 43 |

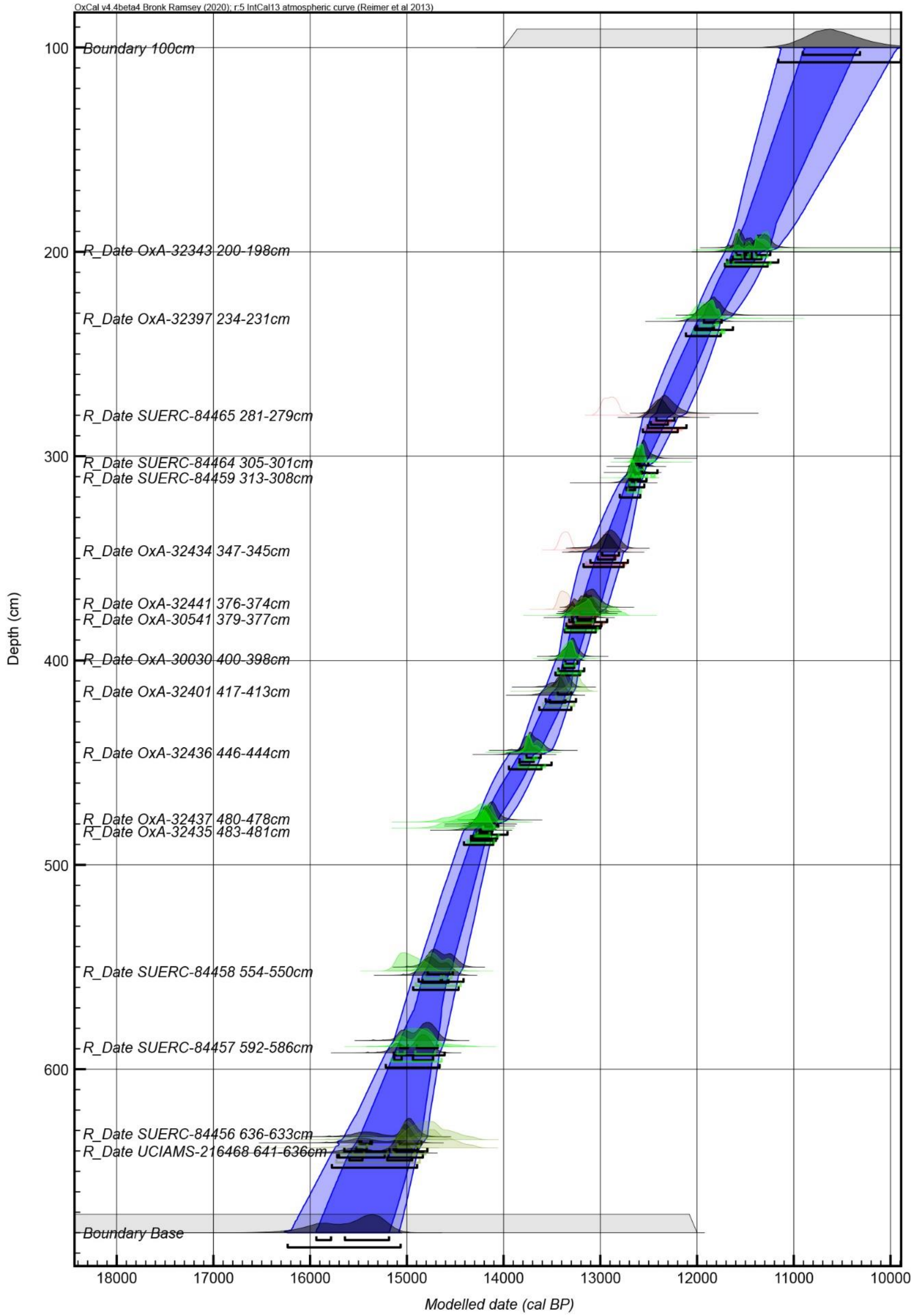


Figure 3. OxCal Bayesian age-depth model from the Wykeham sequence. The dark and light blue envelopes show the modelled 68 % and 95 % confidence intervals respectively. Age ranges are coloured according to their posterior outlier probabilities (green = low, red= high; Table 1).

A Bayesian age-depth model was constructed using a *P_Sequence* deposition model in OxCal v4.4 (Bronk Ramsay, 2008) using the IntCal13 calibration curve (Reimer et al., 2013). The model was run using a variable k factor, allowing the program to objectively determine the model rigidity in order to account for variations in sedimentation rate, and to obtain optimal age-depth relationships (Bronk Ramsey and Lee, 2013). Outlier analysis was performed to objectively down-weight any radiocarbon determinations deemed more likely to be erroneous, applying the 'General' outlier model with a prior outlier probability of 5% to each radiocarbon sample (Bronk Ramsey, 2009). These parameters produced a coherent age model for the sedimentary sequence (Figure 3; Appendices B and C). Three significant outliers (outlier posterior values >70%) were identified from the Outlier model (OxA-32441, OxA-32434, and SUERC-84464; Table 1). These samples contain either poorly preserved *Carex* achenes and/ or twigs which, in some instances, have the potential to produce erroneously older ages via reworking prior to final deposition (e.g. Turney et al., 2000; Walker et al*.,* 2003). Sedimentological data from the dated strata support this interpretation, showing evidence for high levels of allogenic inwash (section 5.1), which may have eroded and re-deposited pre-existing organic deposits surrounding the basin (section 5.2). Modelled ages are reported as mean values ± σ ka BP, and the age model coding and output, including 68.2 % and 95.4 % ranges are included in Appendices B and C respectively. The age-depth model ranges from 15.59 ± 0.32 cal ka BP at 680 cm to 10.56 ± 0.31 cal ka BP at 100 cm (Figure 3).

### 3.3. **Reconstructing past lake-levels**

The principal control on temperate lowland lake levels are rates of groundwater recharge, controlled via rates of catchment precipitation (P) and evaporation (E) (Battarbee, 2000; Cohen, 2003). High lake-levels represent a positive P-E balance, whilst lower lake-levels represent a negative P-E balance (Harrison and Digerfeldt, 1993; Magny et al., 2007). The Wykeham palaeolake was formed in a topographic depression within permeable glacifluvial sediments and therefore the palaeolake level reflects the eastern VoP groundwater elevation which is controlled principally by meteoric recharge (Carey and Chadha, 1998; Brown et al., 2011). Therefore, variations in the palaeolake level reflect shifting rates of P and E, with high (low) lake levels invoking increased (decreased) rates of groundwater recharge under relatively humid (arid) hydroclimates.

Palaeolake-levels were reconstructed using the sedimentological, macrofossil, and isotopic datasets, which together show evidence for shifts from sublittoral lacustrine (high) to eulittoral (low) conditions through the LGIT, a process that can be separated from hydroseral succession by the revertence to sublittoral/ lacustrine conditions expressed in the overlying sediments. High relative lake-level phases are reconstructed using the following lines of evidence: a) lacustrine lithofacies indicating deposition within a standing water body, b) macrofossil assemblages dominated by aquatic flora and fauna, c) $\delta^{13}C_c$ values between +3 and -3 ‰, indicative of lacustrine carbonates (Talbot, 1990), and d) decoupled $\delta^{18}O_c$ and $\delta^{13}C_c$ values, indicating an open lake system (Leng and Marshall, 2004). Low relative lake-level phases are reconstructed by: a) eulittoral lithofacies and b) macrofossil assemblages dominated by eulittoral taxa. In line with other evidence, $\delta^{13}C_c$ values lower than -3 ‰ may also indicate low lake-level phases and the formation shallow/paludal water bodies with high vegetation cover (Talbot, 1990; Alonso-Zarza, 2003; Candy et al., 2015; discussed further in section 5.3.2).

Table 2. Macrofossil water depth ranges used to reconstruct the maximum water depth. *P. filiformis* and *P. pusillus* ranges derive from Spence and Chrystal (1970) and Dieffenbacher-Krall and Haltemann, (2000) respectively. All other ranges are derived from Hannon and Gaillard (1997).

| Taxa | Water depth ranges (m) |
|---|---|
| *Chara* thalli. | <4-6 |
| *Myriophyllum spicatum* | 1-5 |
| *Potamogeton filiformis* | *<1.5* |
| *Potamogeton pusillus* | *<1.5* |
| *Equisetum fluviatile* | 0-1 |
| *Phragmites australis* | 0-2 |
| *Typha latifolia* | 0-1 |
| *Juncus* undiff. | 0-1 |
| *Carex* undiff. | 0-1 |

With the exception of charophyte gyrogonites/ oospores, the seeds and fruits of most aquatic taxa are not widely dispersed from their parent plants, meaning that their presence in the macrofossil record represents the aquatic vegetation in close proximity to the sampling site (Zhao et al., 2006). The Wykeham basin is a first order lake with a restricted catchment, a single spring-fed river input of less than 300 m length and direct coupling to the surrounding slopes (Figure 1), supporting our inferences for local groundwater changes. Therefore, by using maximum depth niches of the aquatic and wetland macrofossil taxa (Hannon and Gaillard, 1997), an estimate of the maximum water depth at the sampling site can be calculated and used to estimate shifts in the maximum groundwater elevation (Table 2). The results were constrained to altitudinal data using core depths and absolute altitudinal benchmarks (the Wykeham sequence extends between 19.58 and 25.38 mOD, 6.80 to 1.00 m below the contemporary land surface). An upper groundwater level constraint of 25.50 mOD was employed as no subaqueous deposits have been identified above this elevation in the Wykeham basin, elsewhere in Wykeham Quarry (Lincoln et al., 2017), or at Palaeolake Flixton

(Taylor, 2011; Palmer et al., 2015). The final lake-level reconstruction was linearly detrended to account for the reduction in accommodation space as the basin infilled.

## 4. Results

The Wykeham basin sedimentary sequence is composed of four lithofacies (LF-1-4) consisting of interbedded carbonate-rich silty sands, peats and siliclastic-rich silts, sands and gravels (Table 3 and Figure 2). Using the sedimentology, plant macrofossil, and stable isotope results, and the age-depth model (section 3.1-3.2), the sequence is divided into 8 units (WU-1-8; Figure 2), which are described below.

Table 3. Summary of the Wykeham sequence lithofacies and the units (WU-) in which they are present.

| Lithofacies (LF) | LF codes | WU- | Description | Process interpretation | Depositional environment |
|---|---|---|---|---|---|
| 1 | Sm | 1 | Medium to fine grained minerogenic sand with isolated gravel clasts | Gravity flows in shallow water | Unstable gravel margins on the sides of depressions causing gravity flows into shallow water bodies: **Lacustrine** |
| 2 | Fm, Fl, Sm | 2a, b, c, 4, 5, 6a | Carbonate-rich massive to faintly laminated silty, friable fine sand with abundant carbonate thalli casts of *Chara sp.,* isolated gastropod shells and isolated fine gravel clasts (Appendix A). | Still-slow-flowing water authigenic sedimentation in base-rich lakes | Spring-fed freshwater charophyte meadows on sublittoral lake benches (<4-6 m mean water depth): **Lacustrine** |
| 3a | Fm; Sm; | 3, 6b, 7b | Siliclastic-rich sandy clayey silt interbedded with laminations to beds of fine to coarse sands | Low energy suspension settling of allogenic material in shallow water depths | Shallow oligotrophic water-bodies with limited vegetation cover in either the catchment or within the lake: **Lacustrine** |
| 3b | Sm: Gm | 7a | Siliclastic-rich fine-coarse sands and moderately to poorly sorted fine to medium gravels including limestone. | High energy inflows either via gravity flows or slumping of gravels from unstable basin margins during intervals of low relative lake-level | High energy and unstable catchment conditions in the absence of perennial standing water: **Eutlittoral/ Terrestrial** |
| 4 | C; Fm | 4, 8 | Poorly to well humified silty peat irregularly interbedded with LF-2 | Marginal accretion of organic detritus either where peat was submerged for long periods (poorly humified), or at higher elevations, being predominantly sub-aerially exposed (well humified) | Eulittoral marsh/ backswamp environments (< 1 m mean water depth) at the margins of water bodies: **Eulittoral** |

### 4.1. **WU-1 (680-676 cm; 15.59 ± 0.32 to 15.55 ± 0.31 cal ka BP)**

WU-1 is the basal unit of the Wykeham sequence and is comprised of well- to moderately sorted, sand-rich siliclastic material, with gravel clasts including oolitic limestone (LF-1). The deposits are comprised principally of siliclastic content (57 %), whilst carbonate and organic content is comparatively low compared to the overlying strata (< 40 % and 3 % respectively).

A single macrofossil sample obtained from WU-1 contained only charophyte oospores (Figure 4). No additional proxy data were obtained from these deposits.

### 4.2. **WU-2 (676-472 cm; 15.55 ± 0.31 to 14.05 ± 0.09 cal ka BP)**

WU-2 is divided into three sub-units: WU-2a (676-638 cm; 15.55 ± 0.31 to 15.20 ± 0.26 cal ka BP), WU-2b (638-568 cm; 15.20 ± 0.26 to 14.78 ± 0.13 cal ka BP) and WU-2c (568-472 cm; 14.78 ± 0.13 to 14.05 ± 0.09 cal ka BP). Collectively, the WU-2 deposits consist of well-sorted carbonate-rich silty sands containing high abundances of calcified charophyte thalli encrustations (LF-2). Carbonate content fluctuates between 33 and 83 % in WU-2a-2b, steadily rising through these units whilst siliclastic content lowers from 65 to 15 %. In WU-2c, carbonate content is consistently high (>70 %, reaching peak values of 82 %) and siliclastic content is low (15-30 %). Organic content is low throughout WU-2 (< 4 %). The WU-2 thin sections show that carbonate content is derived principally from calcitic micrite within the sediment matrix (groundmass) and microspar crystals precipitated around charophyte thalli (Appendix A).

The WU-2 aquatic macrofossil assemblage is dominated by two types of charophyte remains (Figure 4). In WU-2a, charophyte oospores dominate the aquatic assemblage but are replaced by calcified charophyte thalli casts in WU-2b which then dominate the assemblage. Other aquatic macrofossils consist of *Potamogeton filiformis* and *Myriophyllum spicatum* seeds which are present in low abundances in WU-2b. Eulittoral species diversity is low, with only *Juncus* undiff. seeds and moss leaves and stems including *Drepanocladus, Scorpidium scorpioides* and *Barbula recurvirostra* identified. Terrestrial remains consist of perennial herbs (Poaceae, *Taraxacum cf. officianale, Rumex acetosella, Potentilla erecta*) and dwarf shrubs (*Empetrum nigrum, Betula nana* and *Salix* undiff.).

$\delta^{18}O_c$ values are low at the base of the sequence but rise by +1.46 ‰ to -6.32 ‰ in WU-2a (Figure 5). In WU-2b, $\delta^{18}O_c$ values initially oscillate from -6.32 ‰ to -7.51 ‰, and then remain high and stable ($\delta^{18}O_c$ mean = -6.65‰, 1σ = 0.12‰) before steadily declining by ~-1.50 ‰ to -8.10 ‰ in WU-2c. The $\delta^{13}C_c$ values are initially high in WU-2a (+1.32 ‰) and become steadily lower through WU-2b-2c, reaching a minimum value of -2.50 ‰ at 478 cm. The different trends in $\delta^{18}O_c$ and $\delta^{13}C_c$ in WU-2 demonstrate that the values are decoupled ($r^2$= 0.03).

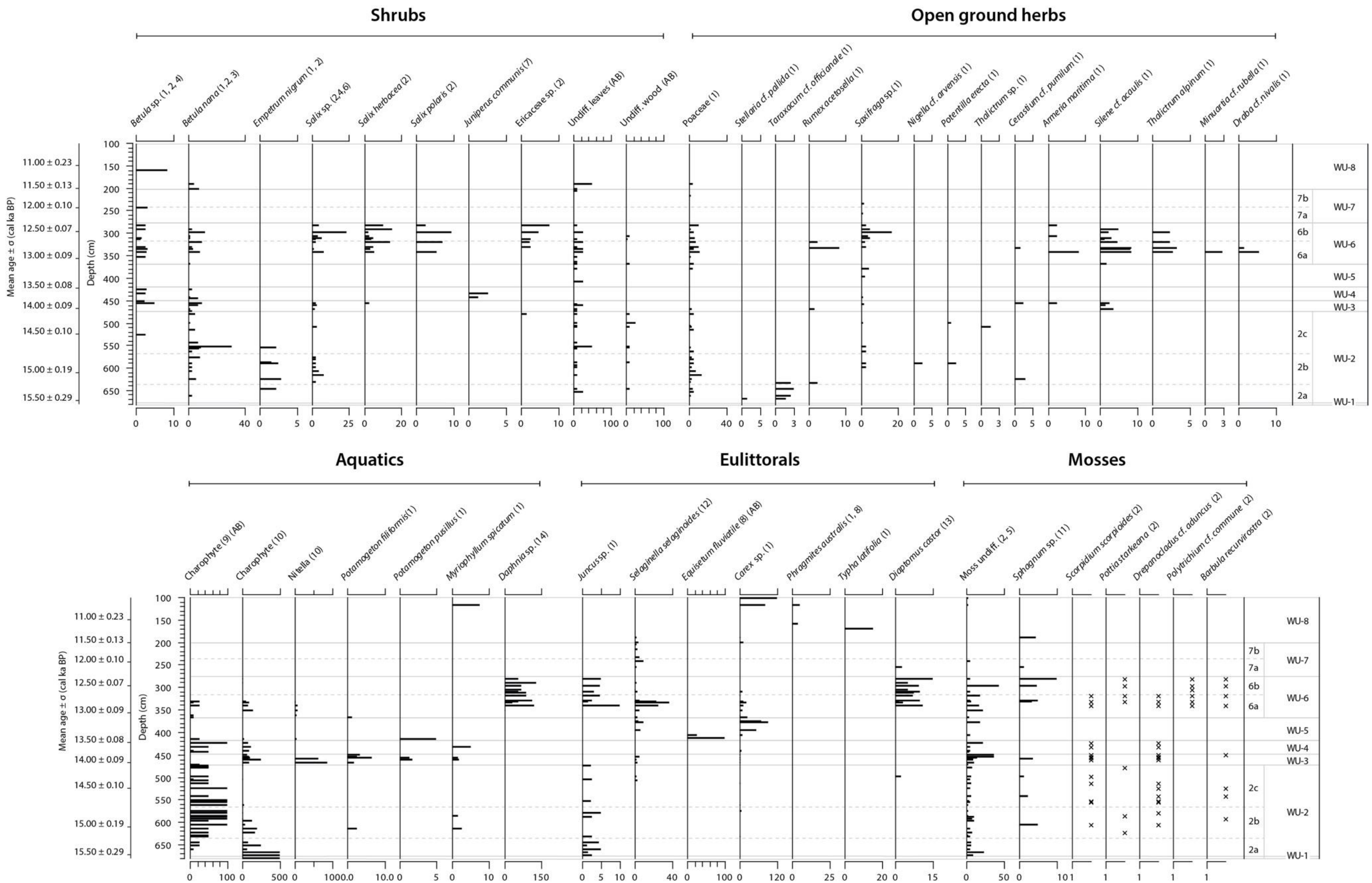


Figure 4. Macrofossils from the Wykeham sequence. (1) seeds/ fruits/ achenes, (2) leaves, (3) catkins, (4) twigs, (5) stems, (6) budscales, (7) needles, (8) rhizomes, (9) calcified thalli, (10) gyrogonites/ oospores, (11) sporangia, (12) megaspores, (13) egg sacs, (14) ephippia. (AB) denotes taxa counted using the abundance scale (section 3.1).

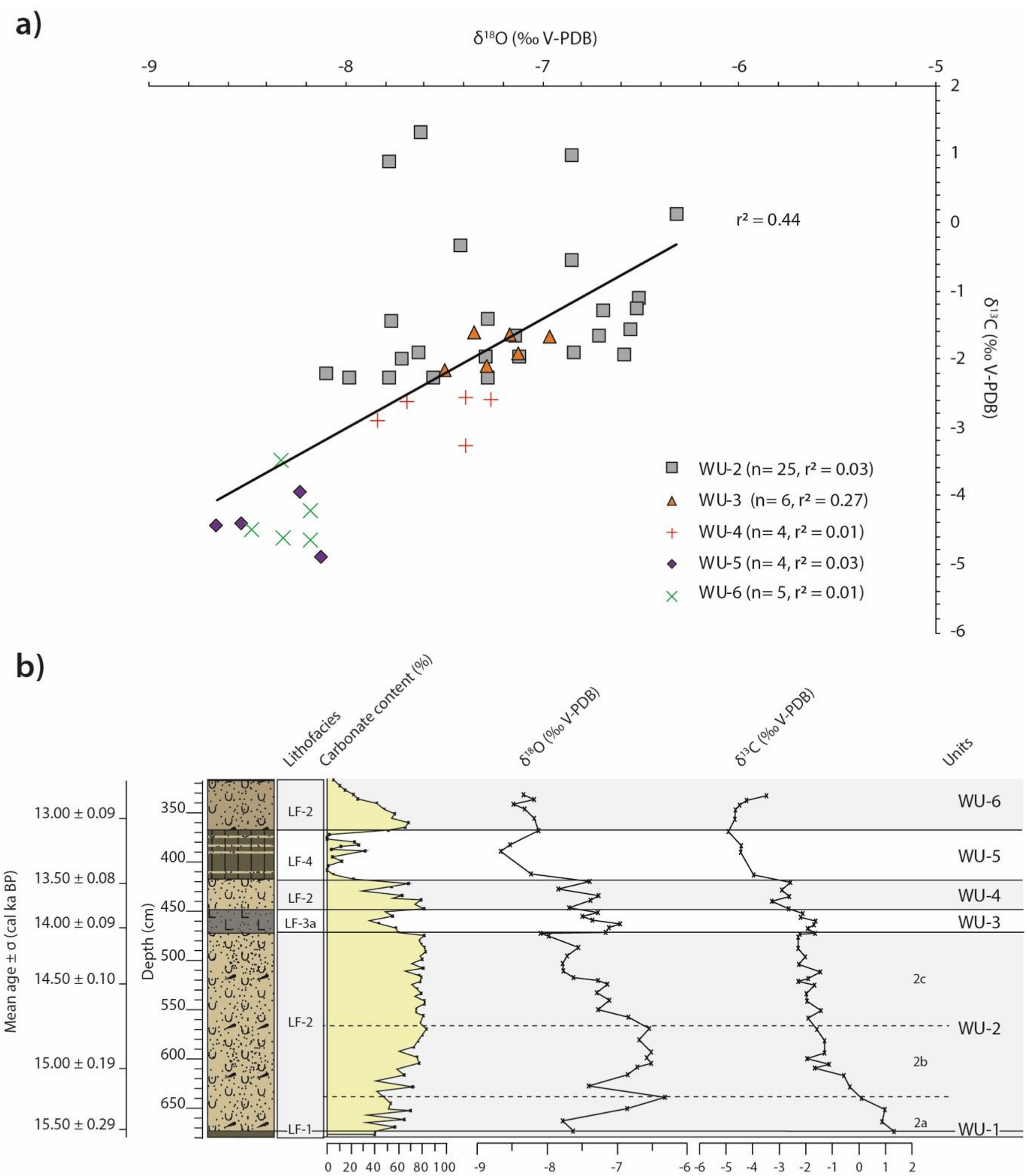


Figure 5. a) Comparison of the $\delta^{18}O_c$ and $\delta^{13}C_c$ values from the Wykeham sequence. b) Stratigraphic plot of the $\delta^{18}O_c$ and $\delta^{13}C_c$ values illustrating the lithofacies, stratigraphy and carbonate content through the sequence (from Figure 2) and the Wykeham units. Note that WU-6b, WU-7, and WU-8 are not displayed as no isotopic samples were taken from these units.

### 4.3. **WU-3 (472-448 cm; 14.05 ± 0.09 to 13.79 ± 0.08 cal ka BP)**

WU-3 is characterised by well-sorted, siliclastic-rich, fine sandy silts with isolated gravel clasts and moss-rich laminae (LF-3a; Table 3). Carbonate (siliclastic) content is significantly lower (higher) than WU-2c (carbonate mean = 50 %, siliclastic mean = 46 %), and organic content remains low (<10 %; Figure 2a). Charophyte thalli are absent from the WU-3 aquatic macrofossil counts and are replaced by charophyte gyrogonites and other lacustrine taxa including *Potamogeton filiformis, Potamogeton pussilus* and *Myriophyllum spicatum*. Although small fragments of charophyte thalli casts were identified in the thin sections in WU-3, their fragmented and incomplete preservation is attributed to their absence in the macrofossil assemblage. Wetland/ damp ground taxa consist of clubmoss megaspores (*Selaginella selaginoides*) and other moss remains (including *Drepanocladus* undiff.). Terrestrial taxa consist of *Betula nana*, *Salix* sp., and upland perennial herbs including *Silene cf. acaulis., Rumex acetosella,* and *Armeria maritima*. $\delta^{18}O_c$ and $\delta^{13}C_c$ rise at the base of WU-3 and remain higher than the mean isotopic values in WU-2c ($\delta^{18}O_c$ mean = -7.33‰, 1σ = 0.20‰; $\delta^{13}C_c$ mean = -1.97‰, 1σ = 0.28‰) although the range of values is entirely consistent with the basal 6 samples in WU-2c (Figure 5).

### 4.4. **WU-4 (448-417 cm; 13.79 ± 0.08 to 13.46 ± 0.08 cal ka BP)**

The WU-4 deposits are composed of LF-2 (Table 3). These deposits are carbonate-rich (30 to 80 %, mean = 58 %) and also contain a higher organic content than the underlying strata. Siliclastic content is lower than WU-3 but rises from 15 % to 46 % through the unit. The aquatic macrofossil assemblage is dominated by charophyte thalli with only a single horizon also containing *M.spicatum* seeds at the top of the zone. Wetland/ eulittoral taxa are largely absent from WU-4, with only low numbers of trigonous *Carex* achenes recorded at 441 cm. Terrestrial remains consist principally of shrub species including *Juniperus communis* needles (present at the base of the zone), *Betula nana* fruits and *Betula undiff.* twigs and fruits (which in some instances appear hybridized). $\delta^{18}O_c$ and $\delta^{13}C_c$ isotopic values in WU-4 are lower than those in WU-3 ($\delta^{18}O_c$ mean = -7.53 ‰, 1σ = 0.13 ‰; $\delta^{13}C_c$ mean = -2.77‰, 1σ = 0.30 ‰).

### 4.5. **WU-5 (417-367 cm; 13.46 ± 0.08 to 13.07 ± 0.10 cal ka BP)**

WU-5 consists of organic-rich silts and poorly humified herbaceous peats (LF-4) which are interbedded with thin (0.5-2 cm thick) carbonate-rich silty laminae (LF-2). Carbonate content varies between 0 and 32 %, whilst organic and siliclastic content reach peak values of 66 % and 67 %, respectively. Sublittoral aquatic taxa are absent from the WU-5 samples with the macrofossil assemblage comprising of mainly eulittoral taxa including *Equisetum fluviatile* rhizomes, *Carex* sp. achenes and pleurocarp mosses including *Scorpidium scorpioides*. Terrestrial species are limited to low numbers of poorly preserved *Betula* sp. fruits, Poaceae seeds, *Selaginella selaginoides* megaspores, and perennial herbaceous taxa including *Silene* cf. *acaulis*. Mean $\delta^{18}O_c$ and $\delta^{13}C_c$ isotopic values from the LF-2 laminae within WU-5 are lower than underlying deposits ($\delta^{18}O_c$ mean = -8.39 ‰, 1 σ = 0.25 ‰; $\delta^{13}C_c$ mean = -4.43 ‰, 1 σ = 0.39 ‰) with $\delta^{18}O_c$ values lowering by -1.26 ‰ from WU-4.

### 4.6. **WU-6 (367-276 cm; 13.08 ± 0.10 to 12.29 ± 0.10 cal ka BP)**

Based upon lithofacies changes, WU-6 is split into two sub-units (WU-6a-WU-6b). WU-6a (367-317 cm; 13.08 ± 0.10 to 12.72 ± 0.06 cal ka BP) consists of LF-2 deposits that are overlain by LF-3a deposits consisting of well-sorted silt-sand-rich siliclastic deposits with (0.5-2 cm thick) fine sand laminae and infrequent fine gravel clasts (WU-6b; 317-276 cm; 12.72 ± 0.06 to 12.29 ± 0.10 cal ka BP). Carbonate content steadily declines through WU-6a (from 68 % to 10 %) and remains below 10 % in WU-6b. Siliclastic content mirrors the carbonate content (increasing from 26 % to 94 % through WU-6a-6b) and organic content ranges between 2 % and 12 %.

Aquatic macrofossil taxa including calicified charophyte thalli casts and oospores re-appear at the base of WU-6. The calcified charophyte thalli however, are only present within the basal 36 cm of the sub-unit, and are frequently broken before becoming absent above 331 cm. Aquatic fauna (*Daphnia* sp. epphipia and *Diaptomus castor*) are present sporadically at the base of the unit and increase in abundance above 340 cm as carbonate content declines < 30 % and siliclastic content increases to > 60 %. Low numbers of eulittoral taxa including *Carex* undiff., *Juncus* undiff., and *Sphagnum* undiff. sporangia are also recorded throughout WU-6. Terrestrial macrofossils are composed principally of open ground herbs (Poaceae, *Saxifraga cf. granulata*. *Silene cf. acaulis*, *Armeria maritima* and *Thalictrum cf. alpinum*), although remains of *Betula* sp. (including *Betula nana*) and *Salix herbacea* (leaves and petioles) are also present in low frequencies. $\delta^{18}O_c$ and $\delta^{13}C_c$ isotopic values in WU-6a remain low ($\delta^{18}O_c$ mean = -8.30 ‰, 1 σ = 0.12 ‰; $\delta^{13}C_c$ mean = -4.30 ‰, 1 σ = 0.49 ‰). No stable isotopic samples were taken from WU-6b (section 3.1).

### 4.7. **WU-7 (276-200 cm; 12.29 ± 0.10 to 11.50 ± 0.13 cal ka BP)**

Based upon lithofacies changes, WU-7 is sub-divided into two sub-units (WU-7a-WU-7b). WU-7a (276-237 cm; 12.29 ± 0.10 to 11.95 ± 0.09 cal ka BP) consists of normally and reverse graded sands and fine gravels interbedded with medium to fine silty sands (LF-3b). Carbonate content ranges between 4 % to 19 %, which from thin section analysis, principally reflects detrital limestone incorporated within the sand and gravel facies (section 3.3). Above 237 cm (WU-7b; 11.95 ± 0.09 to 11.50 ± 0.13 cal ka BP), deposits revert to LF-3a. These deposits consist almost entirely of siliclastic content (> 80 %) with carbonate and organic content below 10 %. Macrofossil concentrations are low throughout WU-7 and identifiable terrestrial macrofossils are confined to *Saxifraga* undiff. seeds and *Betula* sp. fruits which are poorly preserved. Wetland and aquatic species diversity in the macrofossil samples is also low, with only *Selaginella selaginoides* megaspores*,* *Juncus* undiff. seeds and *Chara* gyrogonites recorded. No stable isotopic samples were taken from WU-7.

### 4.8. **WU-8 (200-100 cm; 11.50 ± 0.13 to 10.56 ± 0.31 cal ka BP)**

WU-8 consists of organic-rich silt grading into poorly to moderately humified silty herbaceous peat above 194 cm (LF-4). Organic and siliclastic contents rise from 10 % to over 80 % and fall from 90 % to 20 % respectively between 200 and 140 cm, whilst carbonate is negligible (<2 %) throughout WU-7. The macrofossil assemblage consists primarily of eulittoral taxa with a low species diversity (trigonous *Carex* achenes, *Typha latifolia*, and rhizomes of *Phragmites australis*). Terrestrial macrofossil remains are low in frequency and include *Betula nana* leaves and Poaceae seeds. Aquatic macrofossil taxa are absent from WU-8 with the exception of *Myriophyllum spicatum* seeds at 118 cm. No stable isotopic samples were taken from this unit. Although no sediments were obtained above 100 cm, records from elsewhere in the basin contain sediments analogous to WU-8 that extend to the contemporary land surface (Figure 1d).

## 5. Interpretation

### 5.1. **Sedimentology**

The Wykeham lithofacies reflect deposition within sublittoral/ lacustrine- (LF-1,2,3a) to eulittoral- (LF-3b, 4) environments (Table 3). Charophyte-rich carbonates (LF-2) in WU-2-5a reflect sedimentation dominated by authigenic calcium carbonate precipitation upon a sublittoral lake bench slope (Murphy and Wilkinson, 1980; Treese and Wilkinson, 1982). Low siliclastic and organic content in these deposits invokes a sub-aqueous depositional environment with limited allogenic inwash from the catchment and sedimentation dominated by carbonate precipitation around charophyte thalli and within the water column as a consequence of photosynthesis in *Chara* meadows during summer months (McConnaughey, 1991; Hammarlund et al*.,* 2003). These sediments are characteristic of *Chara* marl lakes in the British Isles (Pentecost, 2009), with carbonate precipitation occurring within groundwater-fed, Ca-rich waters in the basin (section 3.3).

Siliclastic sands, silts, and clays (LF-1 and LF-3a) are indicative of low organic productivity within the water body and surrounding catchment, with fine-grained deposits falling from suspension during periods of limited turbulence in the water column (Palmer et al*.,* 2015). Carbonate content in these lithofacies is derived principally from fragmented charophyte thalli and intraclasts, indicating that they are not *in situ*, and have been eroded/ reworked prior to final deposition. Coarse-grained siliclastic beds (LF-3b) are indicative of high energy processes delivering allogenic sediment into the topographic depression either via subaerial exposure and slumping of the basin margins (Ashley, 1975), and/or flood inflow events

(Schilleref et al*.,* 2015) with limited organic content in either the depression or surrounding catchment. Coarse particle sizes and the lack of interbedded subaqueous deposits suggests that LF-3b represents phases of low relative lake-levels in the depression and the absence of perennial standing water in WU-7a (section 5.4).

Organic-rich silty peat (LF-4) represents deposition in close association with the mean water level in an eulittoral depositional environment. Laminae of LF-2 in WU-5 suggests shifts in the relative lake-level, frequently switching between eulittoral and sublittoral/ lacustrine conditions. The steady increase in organic content in WU-8 invokes the final infilling of the water body via hydroseral succession.

## 5.2. **Macrofossils**

Aquatic and eulittoral macrofossils in the Wykeham sequence represent vegetation growing within or at the margins of the palaeolake respectively (section 5.4). The terrestrial macrofossil assemblage reflects flora growing locally within the catchment and entering the palaeolake body either via direct airfall or streamflow. The small size of the Wykeham basin and the spring inflow provide significant potential for the influx of terrestrial macrofossils into the basin. Low abundances of terrestrial macrofossils recovered in WU-5, WU-7, and WU-8 are interpreted to reflect a taphonomic bias during intervals of low relative lake-level and limited inflow (section 5.4). The macrofossils within these units therefore only reflect terrestrial taxa growing directly within or at the margins of the Wykeham basin.

The following trends are identified in the terrestrial macrofossil assemblage. In WU-2 and WU-3, the assemblage is characteristic of an open steppic landscape, with limited shrub cover (*Betula nana, Salix* sp. and *Empetrum nigrum*) in the VoP lowlands between 15.55 ± 0.31 and 13.79 ± 0.08 cal ka BP. Disturbed ground- and montane taxa (*Rumex acetosella* and *Silene c.f. acualis* respectively) in WU-3 suggest a temporary niche change between 14.05 ± 0.09 and 13.79 ± 0.08 cal ka BP, possibly in response to a deterioration in hydroclimatic conditions (section 5.5). Lower abundances of herbs and rises in shrubby taxa (e.g. *Juniperus communis.*) in WU-4 reflect the stabilisation of the landscape between 13.79 ± 0.08 cal ka BP and 13.46 ± 0.08 cal ka BP. The rise in *Betula* sp. remains in WU-4 reflects an expansion in local *Betula* growth in the catchment. No *Betula* remains in the Wykeham sequence can be conclusively assigned to tree species (e.g. *B. pubescens* or *B. pendula*) however, suggesting that for the duration of the Wykeham palaeolake's existence, closed forest cover did not develop in the immediate vicinity of the palaeolake.

The WU-6 and WU-7 assemblage indicates a re-opening of the catchment vegetation cover between 13.08 ± 0.10 and 11.50 ± 0.13 cal ka BP. Open ground herbs and shrubs tolerant of disturbed ground (e.g. *Rumex acetosella*), and late-lying snow cover (e.g. *Salix herbacea*) suggest a deterioration in climatic conditions (section 5.5) and the re-development of open disturbed grassland environs around the Wykeham basin. High macrofossil concentrations in WU-6 coincide with rising allogenic inwash into the basin, indicating enhanced erosion and redeposition of sediments and vegetation from the lake margins into the water body (section 5.1). These processes are thought to explain the apparently old radiocarbon ages from OxA-32441, OxA-32434, and SUERC-84464, redepositing *Carex* macrofossils and twigs from the basin margins (section 3.2). Low terrestrial macrofossil concentrations in WU-7 and WU-8 suggest low catchment vegetation cover during the terminal stages of the palaeolake.

## 5.3. **Stable isotopes**

### *5.3.1. $\delta^{18}O_c$*

It is widely assumed that, in the British Isles, the $\delta^{18}O_c$ value of lacustrine carbonate sequences that span the LGIT are primarily reflecting changes in prevailing air temperature (e.g. Marshall et al., 2002; Van Asch et al., 2012; Candy et al., 2016; Blockley et al., 2018). This assertion is reliant on the following assumptions: 1) that prevailing air temperature exerts a strong control on the $\delta^{18}O$ of rainfall ($\delta^{18}O_r$), with that relationship being +0.58 ‰/+1 °C in the modern day (Rozanski et al., 1992;1993); 2) that the $\delta^{18}O_r$ controls the $\delta^{18}O$ value of groundwater ($\delta^{18}O_g$) and, consequently of lakewater ($\delta^{18}O_l$); 3) that minimal modification of the $\delta^{18}O$ water signal occurs during the recharge of the lake waters; 4) that therefore, changes in air temperature are transferred, through these steps, into changes in $\delta^{18}O_l$. The $\delta^{18}O_c$ of lacustrine carbonates mineralising in these waters will therefore inherit the $\delta^{18}O_l$ signal but are modified by the temperature-controlled isotopic fractionation of -0.24 to -0.28 ‰/ +1 °C that occurs during mineralisation (Hays and Grossman, 1991; Kim and O'Neil, 1997; Leng and Marshall, 2004). Although the temperature control on $\delta^{18}O$ in meteoric waters and isotopic fractionation during mineralisation operate in different directions, increasing under warmer temperatures for the former but decreasing under warm temperatures for the latter, the effect of air temperature on the isotopic value of rainfall is greater and therefore dominates changes in $\delta^{18}O_c$ values (Leng and Marshall, 2004; Candy et al., 2016). This assertion assumes that there is minimal modification of the $\delta^{18}O$ of meteoric waters, by processes such as evaporation, during recharge and the residence time of waters in the lake basin (Leng and Marshall, 2004).

These assumptions are validated by three lines of evidence. First, numerous LGIT $\delta^{18}O_c$ lacustrine sequences show that warmer intervals, such as the early Holocene and the Lateglacial Interstadial are characterised by higher isotopic values than colder intervals, such as the Lateglacial Stadial/ Younger Dryas (e.g. Marshall et al., 2002; Diefendorf et al., 2006; Van Asch et al., 2012). Second, $\delta^{18}O_c$ records from British LGIT sequences show a similar pattern to $\delta^{18}O$ records of the same interval in the Greenland ice cores, i.e. NGRIP, a record where air temperature is considered the driving control of the isotopic signature (Rasmussen et al., 2006). Third, a number of LGIT records from northwest Europe contain independent palaeotemperature estimates based on chironomid-inferred temperatures (C-ITs), which routinely show that variations in $\delta^{18}O_c$ values match the variations seen in reconstructed C-ITs (e.g. Van Asch et al., 2012).

As with other British LGIT lacustrine $\delta^{18}O_c$ records, the isotopic structure of the Lateglacial Interstadial at Wykeham is similar to that of Greenland Interstadial 1 (GI-1) in that: 1) the highest, and, therefore, 'warmest' $\delta^{18}O_c$ values occurring soon after the onset of the Interstadial (WU-2b); 2) there is a trend of decreasing isotopic values as the Interstadial progresses (WU-2c to WU-6); 3) the record shows a similar stratigraphy of warm and cold events as the interstadial record of NGRIP (Rasmussen et al., 2006; 2014). It is important to note, however, that there is no independent record of quantified palaeotemperatures from the Wykeham sequences. Furthermore, the chronology for the Interstadial at Wykeham presented here shows that even though the isotopic stratigraphy of this interval is consistent with that of NGRIP, the timing of some of the warm/cold events are offset. This may, of course, be true of many of the British LGIT $\delta^{18}O_c$ records but very few of them have a chronology as robust as Wykeham which allows this to be tested. Finally, as it is clear from the other data that major changes in lake-level and hydrology have occurred at Wykeham during this time interval (section 5.4), it is possible that the $\delta^{18}O_c$ signal may represent hydrological changes rather than temperature variability. These hydrological changes may include changing lake levels, with smaller more contracted water bodies being more susceptible to evaporation and therefore modification of the $\delta^{18}O_c$ signal, or varying levels of seasonal snow melt which may result in the episodic 'flooding' of the lake basin with waters that have relatively low $\delta^{18}O$ values (see Candy et al., 2016 for discussion). Despite these uncertainties, the following lines of evidence support that prevailing temperatures were one of the dominant controls on the Wykeham $\delta^{18}O_c$ signal.

First, the modern $\delta^{18}O_g$ in the VoP closely matches mean annual $\delta^{18}O_r$ (Bearcock et al., 2016; Appendix D). Therefore, if it is accepted that the lake water in the Wykeham basin was principally groundwater fed (section 2), and carbonates mineralised in isotopic equilibrium with the lake water (Appendix D2), then the resulting $\delta^{18}O_c$ values would relate to the $\delta^{18}O_r$. Second, although no independent temperature record exists in the Wykeham sequence, the palaeolake lies close to the site of Gransmoor (*ca* 25 km SE of Wykeham) which contains one of the most detailed palaeotemperature records for the LGIT, anywhere in the British Isles (Walker et al., 1993). This record, based on the coleopteran mutual climatic range (MCR) technique

(Atkinson et al., 1987), shows the same structure as the Wykeham $\delta^{18}O_c$ record where an initial rise in TMax values to an early peak is followed by a steady decline through the latter half of the Interstadial (Figure 6). Although the initial TMax rise to peak values at the base of the sequence is not precisely chronologically constrained at Gransmoor (Blockley et al., 2004), it occurred prior to the earliest secure date from the sequence at *ca* 14 cal ka BP (Matthews et al., 2017), and is consistent with other coleopteran palaeotemperature records from the British Isles in showing an initial peak in TMax values early in the Interstadial followed by a decline (Atkinson et al., 1987). This supports that the trend of the Wykeham $\delta^{18}O_c$ values is consistent local palaeotemperature trends, which would be expected if the $\delta^{18}O_c$ values were precipitated close to isotopic equilibrium with the $\delta^{18}O_l$, and changes in the VoP $\delta^{18}O_g/\delta^{18}O_r$ were principally controlled by prevailing temperature (see above).

Third, and most significantly, it is possible to compare the $\delta^{18}O_c$ record of Wykeham with that of Interstadial carbonate records from neighbouring Palaeolake Flixton (e.g. Candy et al., 2017; Figure 6). The significance of this comparison is that, whilst the two records are relatively close to each other (Figure 1), and therefore are likely to be affected by similar climatic and hydrological variations, Palaeolake Flixton was significantly larger (*ca* 4.2 km$^2$) than the water body in the Wykeham basin (*ca* 0.03 km$^2$). Consequently, even if the two lakes were exposed to similar hydrological shifts, if hydrology was the main control on the $\delta^{18}O_c$ values, it would be expected that the isotopic record of the two systems would not be comparable. This is because a small water body such as the Wykeham palaeolake would potentially be more strongly influenced by evaporation and snow melt than a large extensive lake system such as Palaeolake Flixton (Leng and Marshall, 2004). When the two records are compared however, the range of $\delta^{18}O_c$ values (Appendix D) and the isotopic stratigraphy of the two records are remarkably similar in regard to the overall trend and the magnitude of major changes in $\delta^{18}O_c$ values (Figure 6). The only point at which the records diverge is in WU-3 in the Wykeham record where $\delta^{18}O_c$ values increase but those in Flixton decline. This can be explained by the fact that between 14.05 ± 0.09 and 13.79 ± 0.08 cal ka BP in the Wykeham sequence, isotopic samples were obtained from LF-3a deposits which are indicative of high allogenic inwash and reworked carbonate fabrics (section 5.1), coupled with a transition to low relative lake levels (section 5.4). It is likely, therefore, that the discrepancy between the $\delta^{18}O_c$ signals during this short interval is a result of different lake sizes with the input of older/reworked carbonate sediments effecting the $\delta^{18}O_c$ at Wykeham but not impacting the larger and deeper Palaeolake Flixton system, where authigenic carbonate continued to accumulate (Palmer et al., 2015). However, the similarity between the two records in terms of the range of values and the isotopic structure is, considering the different bathymetry, areal extent and depth of the two basins, more consistent with a dominant regional control on $\delta^{18}O_c$ (i.e. $\delta^{18}O_r$) rather than localised intralake controls (e.g. hydrological shifts, disequilibrium effects etc.; Leng and Marshall, 2004; Appendix D).

The evidence presented above suggests that, like other British LGIT records, the Wykeham $\delta^{18}O_c$ values reflect the $\delta^{18}O_g$/ $\delta^{18}O_r$ and therefore can be interpreted to reflect changes in prevailing air temperature. Other variables including the amount and seasonality of rainfall, and the distance from the moisture source however can also alter the $\delta^{18}O_r$ (Leng and Marshall, 2004). These variables are typically discounted in other British LGIT records. It is worth noting however, that whilst the earliest part of the Interstadial contains the warmest TMax values in the Gransmoor MCR, it also has the largest TRanges, indicating high seasonality with low winter temperatures and high summer temperatures. In more seasonal climates, cold and extreme winter months are typically drier than the summer months (Denton et al., 2005) due to the fact that warmer air masses can carry more moisture (Rozanski et al., 1993). Therefore, it is likely that during the initial stages of the Interstadial in NE England (i.e. between *ca* 15.20 ± 0.26 and 14.78 ± 0.13 cal ka BP; WU-2b), a greater proportion of annual precipitation occurred during the summer months, when $\delta^{18}O_r$ values are relatively high, rather than the winter months, when $\delta^{18}O_r$ values are relatively low (Darling et al., 2004; Appendix D). Consequently, high seasonality would elevate the $\delta^{18}O_g$/ $\delta^{18}O_c$ values, but this would occur as a result of *both* the seasonality of rainfall and the prevailing temperature of the time interval. The decrease in TRange values from the base of the Gransmoor record shows a steadily declining seasonality signal in NE England in the initial stages of the Interstadial, before stabilising during the latter stages (*ca* 14-13 cal ka BP). The decrease in seasonality would lead to a more maritime hydroclimate, with a more even distribution of rainfall throughout the year, resulting in lower mean annual $\delta^{18}O_r$/ $\delta^{18}O_g$ values. The *ca* -1.5‰ decline in $\delta^{18}O_c$ values between 14.78 ± 0.13 and 14.05 ± 0.09 cal ka BP at Wykeham (WU-2c), and also at Palaeolake Flixton has a similar structure to the decreasing seasonality trend seen in the TRanges at Gransmoor (Figure 6), suggesting that it may represent a decline in the $\delta^{18}O_r$ in response to decreasing seasonality through the early stages of the Lateglacial Interstadial. Together these lines of evidence support that as with other British records, the $\delta^{18}O_c$ values in the Wykeham sequence reflect the $\delta^{18}O_g$/ $\delta^{18}O_r$ of the VoP, which was principally controlled by prevailing air temperatures through the LGIT, but also by the seasonality of rainfall through the initial stages of the Interstadial (i.e. >14 cal ka BP).

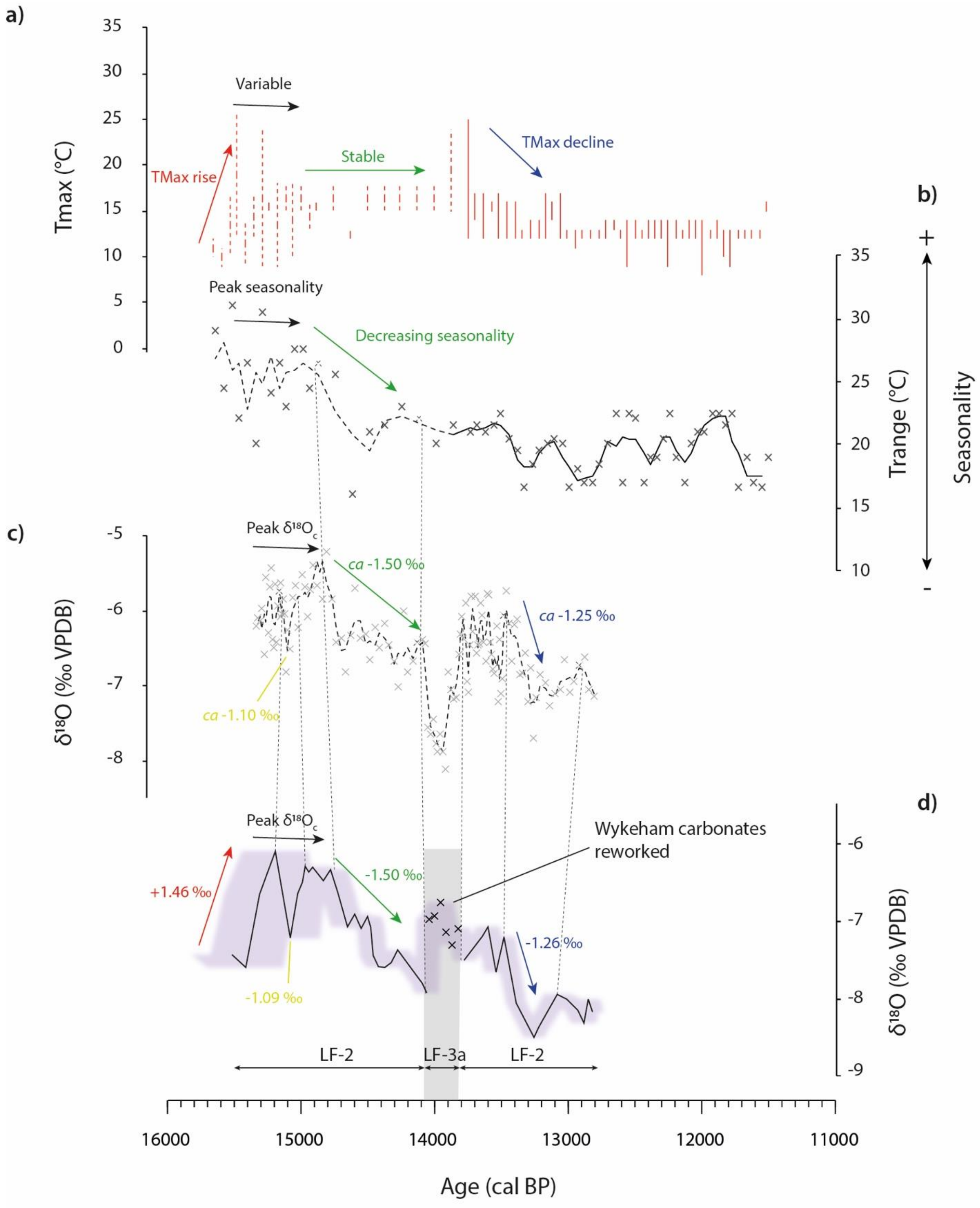


Figure 6. Comparisons between LGIT palaeotemperature and $\delta^{18}O_c$ records from NE England. a) Coleopteran summer /TMax mutual climatic ranges (MCR) from Gransmoor, ca 25 km south of the VoP, dotted ranges indicate values which are not reliably chronologically constrained (Matthews et al., 2017); b) Coleopteran Trange values from the Gransmoor. Crosses mark individual samples whilst the black line represents a three-point moving average through the data. The dotted line represents values which do not have reliable chronological constraints; c) 3-point moving average through $\delta^{18}O_c$ values from basal LGIT marl deposits in Core B at Palaeolake Flixton ca 4 km east of Wykeham (Candy et al., 2017). D) $\delta^{18}O_c$ from the Wykeham basin (this study). As the lowermost records at Gransmoor and the Core B $\delta^{18}O_c$ are not chronologically constrained, correlations have been made between the records (vertical dotted lines) on the basis of similar trends in the proxy records and the magnitudes of major variations (marked by red, black, green and blue arrows).

### *5.3.2. $\delta^{13}C_c$*

In LGIT sequences of northwest Europe, the $\delta^{13}C_c$ values of authigenic lacustrine carbonates are not often used to infer palaeoclimatic change because they are primarily controlled by localised, inter-basin processes. Specifically, $\delta^{13}C_c$ reflects the $^{13}C$ of dissolved inorganic carbon (DIC) composition of the lake water. Lake DIC can be controlled by a number of factors but is primarily a function of the DIC of the water that recharges the lake and uptake/degassing processes occurring within the water body (Leng and Marshall, 2004).

In the Wykeham sequence, $\delta^{13}C_c$ values range between +1.32 and -4.90‰ which are consistent with lacustrine and palustrine calcites precipitated in open lake systems (Talbot, 1990; section 5.3.1). $\delta^{13}C_c$ values are highest at the base of the sequence (WU-2a) before declining by 2.65‰ and then remaining relatively stable between *ca* 15.20 ± 0.26 cal ka BP and 13.79 ± 0.08 cal ka BP (WU-2b to WU-3). This trend of declining $\delta^{13}C_c$ values across the Lateglacial Interstadial is common to many LGIT sequences in the British Isles (e.g. Marshall et al., 2002; Whittington et al., 2015; Candy et al., 2016). Researchers have interpreted this trend as reflecting the progressive increase in soil respired $CO_2$ into the DIC pool of the lake basin as a result of the increase in vegetation density on the landscape as the landscape became recolonised after the Last Glacial Maximum (Candy et al., 2016). Soil respired $CO_2$ has much lower $\delta^{13}C_c$ values than atmospheric $CO_2$ as it is derived from plant respiration and plants strongly fractionate C isotopes in favour of the lighter isotope during photosynthesis. (Cerling and Quade, 1993). The sedimentology and macrofossil evidence from the Wykeham sequences supports this interpretation (sections 5.1-5.2).

During the initial stages of sedimentation (WU-1 to 2), the lake body and surrounding catchment were poorly vegetated. Under these conditions the $^{13}C$ of the lake DIC would have been sourced principally from atmospheric $CO_2$ and the $^{13}C$ enriched limestone geology of the catchment and groundwater aquifer. The transition to lower and relatively more stable $\delta^{13}C_c$ values between *ca* 15.20 ± 0.26 cal ka BP and 13.79 ± 0.08 cal ka BP suggests a progressively higher influx of higher $\delta^{13}C_c$ values into the lake DIC. This transition occurs in phase with a shift to higher and more stable carbonate values in WU-2, and the presence of perennial herbaceous taxa into the sequence, suggesting the development of a more stable and vegetated catchment. This trend continues after 13.79 ± 0.08 cal ka BP where the macrofossil evidence suggests further landscape stabilisation, enhanced vegetation cover and the maturation of catchment soils (section 5.2). The final decrease in WU-5 to values <3 ‰ occurs in conjunction with a lowering of the lake-level (section 5.4), a rise in organic content (section 5.1; Figure 2) and the colonisation of eulittoral taxa in close proximity to the sampling site (section 5.2). These signals suggest the lowering of $\delta^{13}C_c$ reflect a further increase in soil respired $CO_2$ into the lake DIC in response to the expansion of eulittoral taxa into the basin and the decrease in the areal extent of the water body. Similar $\delta^{13}C_c$ signals have been recorded in neighbouring Palaeolake Flixton, where they are interpreted to reflect the transition from a lacustrine into a palustrine/ eulittoral depositional environment (Candy et al., 2015).

### 5.4. **Lake-level changes**

The sublittoral lithofacies and high volumes of charophyte thalli in WU-2 and WU-4 are indicative of deposition in perennial waters no deeper than 4-6 m (Murphy and Wilkinson, 1980; Treese and Wilkinson, 1982; Figure 7; Table 4). Low numbers of other shallow aquatic taxa suggest that WU-2 and WU-4 represent the deepest water facies in the sequence, with peak LGIT groundwater elevations (< 25.50 mOD) obtained between 13.79 ± 0.08 and 13.46 ± 0.08 cal ka BP (WU-3). At the base of the sequence (WU-1 to WU-2a), high volumes of charophyte gyrogonites/ oospores are indicative of high rates of sexual reproduction in shallow water depths (Soulié-Märsche and García, 2015) suggesting that during the initial stages of infill, the lake is shallow (< *ca* 2 m) and possibly susceptible to seasonal dessication, before rising to *ca* 23-24 m OD in WU-2a, perennially submerging the Wykeham depression and enabling clonal vegetative reproduction of the charophyte colonies (WU-2b). In WU-3, charophyte thalli are replaced by gyrogonites/ oospores coupled with *Potamogeton filiformis, P. pusillus* and *Myriophyllum spicatum*, advocating a temporary regression in the water depth to below 1.5 m (*ca* 23.20 mOD) between 14.05 ± 0.09 and 13.79 ± 0.08 cal ka BP (Spence and Chrystal, 1970; Dieffenbacher-Krall and Halteman, 2000). Eulittoral facies (LF-4), coupled with the expansion of eulittoral macrofossil taxa in WU-5 and WU-8 show that the maximum mean water depth was below 1 m above the infill elevation (22.21-22.17 mOD and 24.38-25.38 mOD respectively) between 13.46 ± 0.08 and 13.08 ± 0.10 cal ka BP, and after 11.50 ± 0.13 cal ka BP, respectively. Using the macrofossil taxa alone, water depths are less well constrained between 13.08 ± 0.10 and 11.50 ± 0.13 cal ka BP (WU-6-7). Charophyte thalli in WU-6a are poorly preserved, and frequently fragmented (section 5.1; Appendix A), suggesting unstable conditions in the water column. *Diaptomus castor* egg sacs, moss remains, charophyte gyrogonites and $\delta^{13}C$ values < -3 ‰ (section 5.3) all support shallow (< *ca* 2 m) and ephemeral waters susceptible to seasonal desiccation between 13.08 ± 0.10 and 12.72 ± 0.06 cal ka BP (Bennike, 1988; Talbot, 1990). Gravel facies in WU-7a (LF-3b) indicate intervals of minimal standing water, with the groundwater table lying below the infill elevation of the Wykeham basin (<23.62-24.01 mOD) between 12.29 ± 0.10 cal ka BP and 11.95 ± 0.09 cal ka BP. The re-introduction of sub-aqueous deposits in WU-7b indicate higher effective precipitation regimes in the VoP after 11.95 ± 0.09 cal ka BP but, with limited macrofossil evidence in these sediments, precisely constraining the maximum water depth is not possible. The high and low lake-level phases identified in the Wykeham basin are consistent with other multiproxy based lake-level reconstructions at Wykeham Quarry (Lincoln et al., 2017), and lithostratigraphic reconstructions at Palaeolake Flixton (Palmer et al., 2015), supporting the interpretation that they represent changes in the P-E balance of the VoP groundwater aquifer.

Table 4. Evidence used to reconstruct relative lake-level changes through the Wykeham sequence (section 5.4). Maximum mean water depth is derived from the macrofossil depth niches in Table 2. The water table elevation is calculated from the lake infill elevation + the maximum mean water depth to a maximum elevation of 25.50 mOD (section 3.3).

| WU- | Infill elevation (mOD) | Sedimentology | Dominant macrofossils | Stable isotopes | Maximum mean water depth (m) | Water table elevation range (mOD) |
|---|---|---|---|---|---|---|
| 1 | 19.58-19.64 | LF-1 | Aquatics: charophyte gyrogonites | N/A | *ca* 2 m | |
| 2a | 19.64-20.00 | LF-2: sublittoral facies | Aquatics: charophyte gyrogonites | No co-variance between $\delta^{18}O_c$ and $\delta^{13}C_c$ (open water body) | *ca* 4 m | 21.64-23.92 |
| 2b | 20.00-20.70 | | Aquatics charophyte thalli casts | | *ca* 4 m | 24.05-24.60 |
| 2c | 20.70-21.66 | | | | | 24.70-25.50 |
| 3 | 21.66-21.90 | LF-3a: sublittoral facies | Shallow aquatics: *P.pusillus, P.filiformis, M.spicatum*, absence of charophyte thalli casts | Carbonates reworked & therefore not representative of lake hydrology | *ca* 1.5 m | 23.17-23.38 |
| 4 | 21.90-22.21 | LF-2: sublittoral facies | Aquatics: charophyte thalli casts | No co-variance between $\delta^{18}O_c$ and $\delta^{13}C_c$ (open water body) | *ca 4* m | *ca* 23.90-25.50 |
| 5 | 22.21-22.71 | LF-4: eulittoral facies | Eulittorals: *Equisetum, Carex* | Low $\delta^{13}C_c$ invokes shallow, palustrine conditions | < 1 m | 22.21-23.71 |
| 6a | 22.71-23.21 | LF-2: sublittoral facies | Aquatics-eulittorals: (*D.castor* suggest that standing water may have been ephemeral) | | Estimated < 2 m | 22.71-25.50 |
| 6b | 23.21-23.62 | LF-3a: sublittoral facies | | N/A | | |
| 7a | 23.62-24.01 | LF-3b: eulittoral facies | No dominant taxa, absence of aquatics | N/A | <1 m | <23.62-<24.01 |
| 7b | 24.01-24.38 | LF-3a: sublittoral facies | Eulittorals: (*Carex*), low numbers of charophyte gyrogonites | N/A | 0-2 m | <24.01-25.50 |
| 8 | 24.38-25.38 | LF-4: eulittoral facies | Eulittoral and terrestrial taxa | N/A | <1 m | 24.38-25.50 |

### 5.5. **Synthesis**

Between 15.59 ± 0.32 cal ka BP and 15.20 ± 0.26 cal ka BP, the formation of a topographic depression (kettle hole) initiated the accumulation of sediment within a shallow water body (Figure 8). The basin itself probably formed from the melting of dead ice that remained after the deglaciation of the NSIL in the eastern VoP post *ca* 17.3 ka BP (Evans et al., 2017). The basal age range for the Wykeham sequence indicates that the dead ice here melted within a maximum of *ca* 2 ka. This age range is consistent with the initial infill of other kettle holes in N. Ireland (Watson et al., 2010) and S. Sweden (Wohlfarth et al., 2018), suggesting that dead ice melt and lake formation in the deglaciated outwash plains of the British Isles and Fennosc-

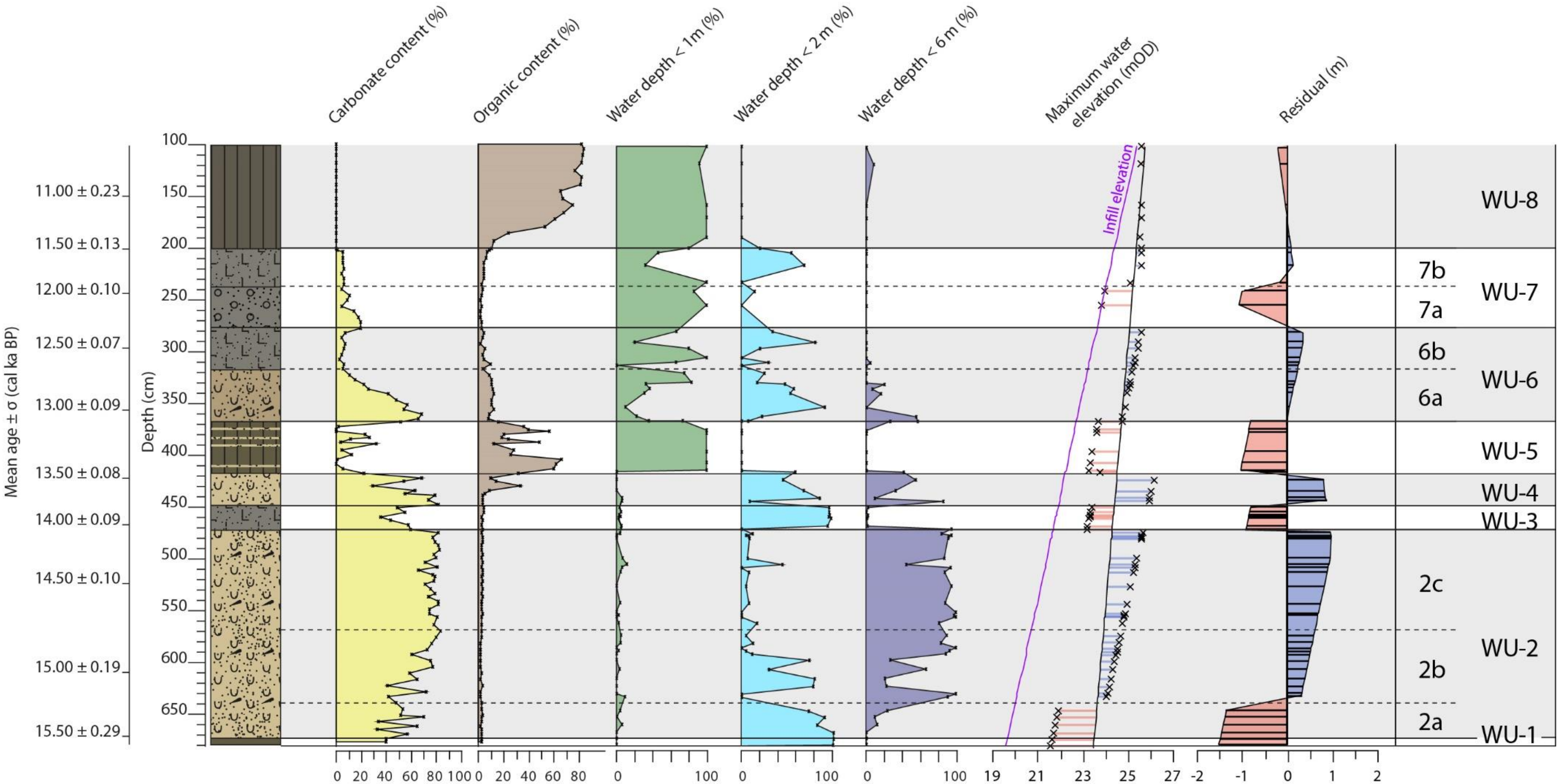


Figure 7. Summary of the sedimentary (lithofacies follows those of Figure 2), and ecological (<1 m, < 2 m and < 6 m water depth % are calculated from the niches of sublittoral-eulittoral macrofossil taxa summarised in Table 4) evidence used to reconstruct relative lake-level changes from the Wykeham sequence. Maximum water elevations (mOD) are calculated from the infill elevation of the Wykeham sequence + the optimum water depth niche of the sublittoral-eulittoral macrofossil assemblage. Positive residuals from a linear smoothing line (grey line) reflect high relative lake-level phases (in blue) and negative residuals (in red) reflect low relative lake-level phases. Mean ages ± σ from the age model (Figure 3) are included for reference

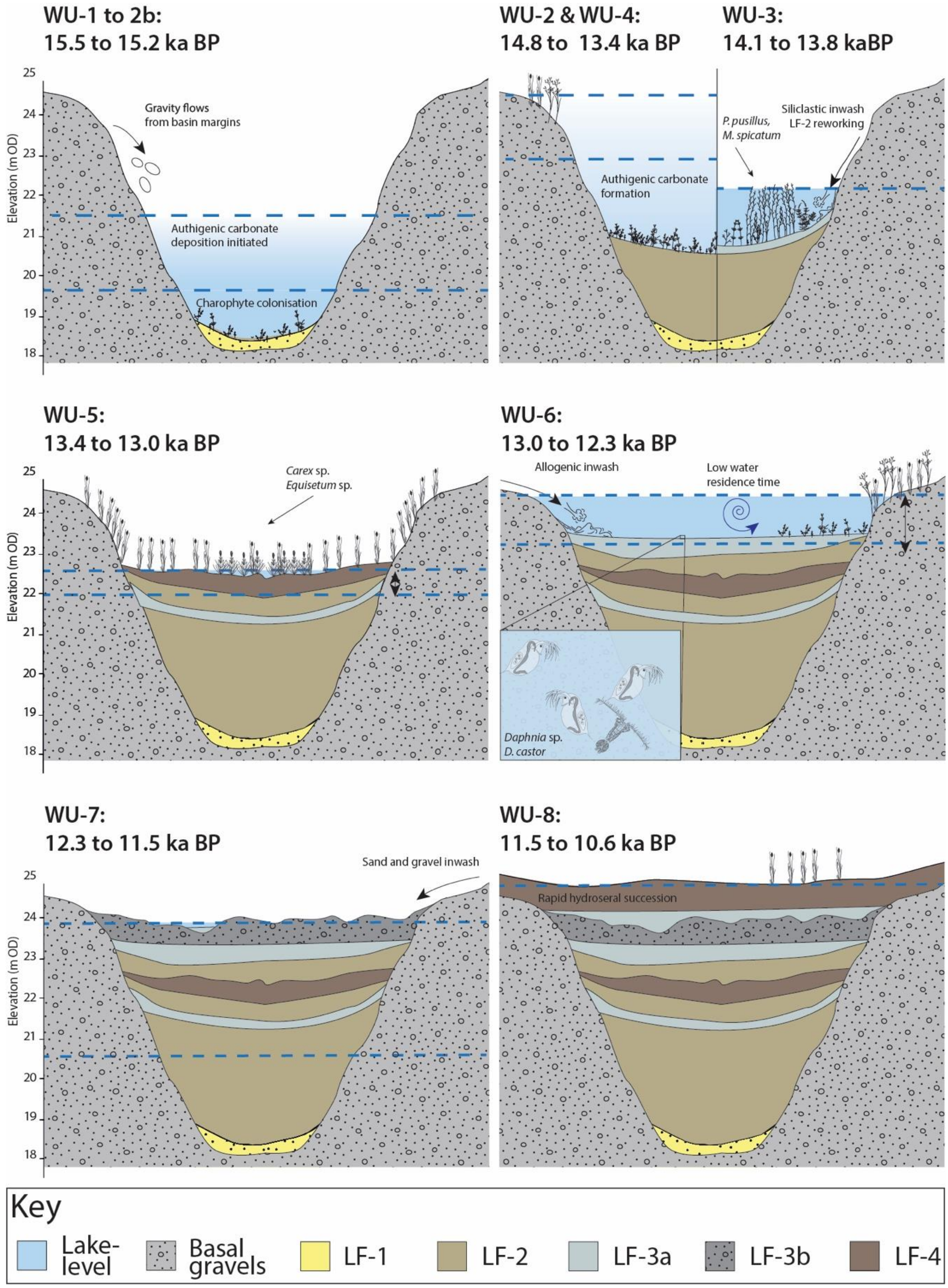


Figure 8. Schematic illustration of the hydrological evolution of the palaeolake, based upon the proxy evidence from WU-1-8. Changes in the lake-level elevation are marked by dashed blue lines.

-andia may have occurred in response to rising summer temperatures after ~16.0 cal ka BP, during the latter stages of Heinrich Stadial 1. Sedimentation in the Wykeham basin was initially dominated by allogenic material (WU-1), but as the water level increased, the lake was colonised by pioneering stands of charophytes which, when coupled with rudimentary perennial herbaceous communities (*e.g. Taraxacum cf. officianale*) and shrubs (e.g. *Empterum* nigrum) in the lake catchment, limited allogenic influx into the lake and facilitated the production of authigenic carbonate.

High $\delta^{18}O_c$ values indicate that summer temperatures were mild in the VoP between 15.20 ± 0.26 and 14.78 ± 0.13 cal ka BP (WU-2b). Similar 'early' spring-summer warming signals to those at Wykeham have also been identified elsewhere in the low and mid-latitudes of Europe (e.g. Genty et al., 2006; Watson et al., 2010; Wagner-Cremer et al., 2011; Samartin et al., 2012; Wohlfarth et al., 2018) suggesting that these hydroclimatic changes reflect an amelioration signal in the European latitudes between 16-15 cal ka BP (Figure 9; Blockley et al., 2004; Buizert et al., 2014; Landais et al., 2018).

At *ca* 14.65 cal ka BP, regional hydroclimatic regimes shifted across the North Atlantic seaboard, causing hemispheric alterations in atmospheric circulation cells and ameliorations in mean annual and, in particular, winter temperatures at the start of GI-1e (Renssen and Isarin, 2001; Steffensen et al., 2008; Rasmussen et al., 2014). Declining $\delta^{18}O_c$ in WU-2c is interpreted to reflect a shift towards a more maritime hydroclimate in the VoP, driven by an amelioration in winter temperature and a reduction in seasonality in NE England (section 5.3; Figure 9). Vegetation cover in the VoP remained relatively open during this interval, with perennial herbaceous communities continuing to persist in the Wykeham catchment between 15.20 ± 0.26 and 14.05 ± 0.09 cal ka BP (section 5.2).

The relative lake-level in the Wykeham basin lowered between 14.05 ± 0.09 and 13.79 ± 0.08 cal ka BP (WU-3), and the sublittoral charophyte meadows at the sampling site were replaced by stands of shallow aquatic flora including *Potamogeton pusillus, P. filiformis* and *Myriophyllum spicatum* in waters no deeper than 1.5 m (Table 4). Allogenic inwash into the lake increased, composed of material eroded from the immediate lake catchment and its margins exposed during lake lowering, and redepositing LF-2 carbonates in the basin (LF-3a; section 5.3). Reductions in temperature (e.g. Matthews et al., 2011), turnovers in palynological and macrofossil assemblages (e.g. Mortensen et al., 2011; Candy et al., 2016), coversand deposition (e.g. Hoek and Bohncke, 2002) and glacial re-advances (e.g. Mangerud et al., 2016; 2017) in Northern Europe and Scandinavia all occurred in phase with the VoP hydroclimatic shifts in WU-3, and are consistent with colder and regionally more arid hydroclimates in these areas during the Older Dryas chronozone (between *ca* 14.1 and 13.9

cal ka BP). These changes occurred in phase with GI-1d in the Greenland ice cores, where a depletion in $\delta^{18}O$ and elevated $Ca^{2+}$ show a climatic deterioration in the high latitudes coupled with regional-to-hemispherical-scale changes in atmospheric circulation (Rasmussen et al., 2014).

Charophyte meadows recolonised the marginal sectors of the water body, as effective precipitation recharging the VoP aquifer drove a rise in the groundwater level to optimum interstadial elevations by 13.79 ± 0.08 cal ka BP. The relative lake-level remained high and the sedimentation rate in the basin declined as accommodation space decreased and stable soils occupied by shrubby taxa developed in the catchment between 13.79 ± 0.08 and 13.45 ± 0.08 cal ka BP. *Juniperus communis* needles at the base of WU-4, represents the development of Juniper scrub in the catchment. The timing of *Juniperus* influx into the Wykeham basin is consistent with the first presence of *Juniperus* macrofossils in other records at Wykeham Quarry (Lincoln et al., 2017), as well as a rise in *Juniperus* pollen at Gransmoor (Walker et al., 1993), suggesting a regional expansion of *Juniperus* in the lowlands of NE England between *ca* 14.00 - 13.70 cal ka BP. This is significant, as rises in *Juniperus* have been widely reported from the palynological records of NE England and assumed to reflect direct landscape responses to the rapid warming at the onset of the Lateglacial Interstadial (e.g. Tweddle, 2001). The macrofossil record from Wykeham Quarry and pollen records from Gransmoor however, demonstrate that the development of *Juniperus* scrub in NE England occurred significantly later than the initial climatic amelioration at the start of the Lateglacial Interstadial, during or soon after the WU-3 hydroclimatic event. Therefore, it is more likely that the expansion of *Juniperus* was driven by increased habitat availability during and/ or soon after the hydroclimatic changes of WU-3 (Abrook, 2017).

Palynological records from the VoP (Day, 1996; Abrook, 2017) and Gransmoor (Walker et al., 1993) show that rises in *Betula* pollen to optimum values, after the initial peak in *Juniperus*, is thought to represent the onset of peak Interstadial woodland cover in the region, and therefore highest landscape stability around *ca* 13.8 ka BP (Matthews et al., 2017). Decreases in the sedimentation rate (Figure 3) and a reduction in $\delta^{13}C_c$ values at Wykeham support a stabilisation of the landscape during this interval (section 5.3). There is no evidence however for the development of extensive tree cover in the vicinity of the Wykeham basin (section 5.2).

At 13.46 ± 0.08 cal ka BP, temperatures declined in the VoP and the groundwater lowered, forming a fen peatland in the basin (WU-5). This occurred in phase with $\delta^{18}O_c$ and C-IT declines in other British (Brooks and Birks, 2000; Marshall et al*.,* 2002; Candy et al*.,* 2016), and European records (e.g. Heiri et al., 2007; Lotter et al., 2012) suggesting a regional climatic deterioration equivalent with GI-1b in Greenland and the Gerzensee oscillation in Europe. A shallow lake reformed at Wykeham by 13.08 ± 0.10 cal ka BP (WU-6a), but air temperatures remained low, with vegetation cover declining as open ground herbs replaced shrubby taxa in the lake catchment and allogenic material from unstable soils were washed into the lake basin. This phase is broadly concomitant with a short interval of $\delta^{18}O$ enrichment in the Greenland ice cores (GI-1a) indicative of a temporary amelioration in temperatures (Rasmussen et al., 2014). No substantial $\delta^{18}O_c$ rise is recorded at Wykeham, suggesting that prevailing temperatures in the VoP did not substantially warm during the GI-1a chronozone.

Northern Hemispheric cooling at the start of the GS-1 chronozone coincided with a reduction in carbonate precipitation in the Wykeham basin. Standing water persisted at least seasonally between 12.72 ± 0.06 cal ka BP and 12.29 ± 0.10 cal ka BP (WU-6b), but biogenic productivity within the water column and the catchment was low, with vegetation cover consisting almost entirely of perennial herbs with arctic and/or montane ecological niches. Involuted interstadial deposits elsewhere at Wykeham Quarry show that perennially frozen ground developed under low mean annual temperatures during this interval (Lincoln et al., 2017). In NW Europe, continuous permafrost formed across the northern British Isles and Scandinavia, and it is possible that this maintained perched groundwater bodies across these regions during the initial stages of the Younger Dryas.

The VoP groundwater fell below the infill elevation of the Wykeham palaeolake at *ca* 12.29 ± 0.10 cal ka BP cal ka BP, promoting the influx of sand and gravel beds from the basin perimeter onto the Wykeham lake bench, and forming hiatuses in the lacustrine records at neighbouring Palaeolake Flixton (Palmer et al., 2015). Any standing water was ephemeral and fed from nival melt and fluvial discharges which temporarily formed a shallow water body within the basin during spring-summer months. It is unclear whether the lower lake-levels were associated with a concomitant shift in temperature, but the low organic content of the sediments, coupled with the absence of any thermophilic macrofossil taxa, suggests that catchment vegetation cover and temperatures remained low. The precise timing of this hydrological change is poorly resolved in the Wykeham age model (Figure 3). At Meerfelder Maar in western Germany (Rach et al., 2014), and Hässeldala Port in southern Sweden (Muschitiello et al., 2015), an abrupt shift to more arid hydroclimates similar to that in WU-7a at Wykeham is recorded at *ca* 12.68 ka (Figure 9). On the basis of the consistency in hydrological signals and the precise chronologies from Meerfelder Maar and Hässeldala Port, it is considered highly likely that the shift to lower lake levels in WU-7a at Wykeham represents a response in the VoP groundwater to this regional hydrological signal. However, without further chronological control and palaeoclimatic data from the VoP, this correlation remains tentative.

Gravel inwash into the basin ceased at *ca* 11.95 cal ka BP, and the groundwater elevation had risen sufficiently in the VoP to reform a shallow water body in the Wykeham depression. Although no temperature evidence is available from Wykeham, the timing of the lake level rise can be compared to climatic records from neighbouring Palaeolake Flixton (Blockley et al., 2018), where a sharp $\delta^{18}O_c$ increase occurs within age error of the rise in the Wykeham lake level (Figure 9). This evidence supports that a rise in groundwater elevation through the VoP basin occurred during the latter stages of the Younger Dryas/ GS-1 chronozone, prior to the hemispheric amelioration in regional temperatures at the start of the Holocene (*ca* 11.65 cal ka BP). It should be noted that whilst temperatures had begun to ameliorate, the landscape remained open and unstable, with only perennial herbs colonising the catchment.

Two abrupt climatic events (ACE-1 and ACE-2) have been recorded in the Early Holocene records at Palaeolake Flixton (Figure 9) which impacted air temperatures, and ecosystems in the VoP (Blockley et al., 2018). ACE-1 occurred within age uncertainty of the infilling of the lake and the development of fen peat in the Wykeham depression at 11.50 ± 0.13 cal ka BP (WU-8). This event is broadly contemporaneous with the 11.4 ka event in the Greenland ice cores (Rasmussen et al., 2014). It is likely that the climatic deterioration recorded in Palaeolake Flixton promoted a temporary reduction in the groundwater elevation during an interval of lower effective precipitation regimes (e.g. Magny et al., 2007), causing the rapid infill/ hydroseral succession of the Wykeham lake. ACE-2 occurred after the lake had infilled, meaning that no supporting evidence for hydroclimatic changes associated with this climatic oscillation are available from the Wykeham basin.

## 6. Regional heterogeneity in hydroclimate

The record from the Wykeham basin demonstrates that hydrological changes accompanied abrupt climatic events during the LGIT but did not always occur in phase with Greenlandic temperature variations. This is notable in the initial amelioration signals (formation of the Wykeham basin, precipitation of authigenic carbonates, and rising $\delta^{18}O_c$ values) at the base of the Wykeham basin sequence (WU-1 to 2a), which suggests that the VoP was becoming at least seasonally warmer and wetter prior to the abrupt amelioration in Greenland at the start of GI-1e (Figure 9). These reconstructions are in agreement with a series of other European palaeoclimatic records which indicate warming prior to the start of GI-1e (e.g. Walker et al., 2003; Watson et al., 2010; Shakun et al., 2012; Wohlfarth et al., 2018), although in most instances, these archives have less secure chronologies than the Wykeham sequence, limiting secure regional correlations. Hydrological changes (rising lake levels) also appear to have been initiated in the VoP *ca* 0.3 ka prior to the onset of the Holocene at *ca* 11.65 cal ka

BP. Together, these signals support a repeated regional asynchrony in hydroclimatic responses to the two major warming intervals of the LGIT.

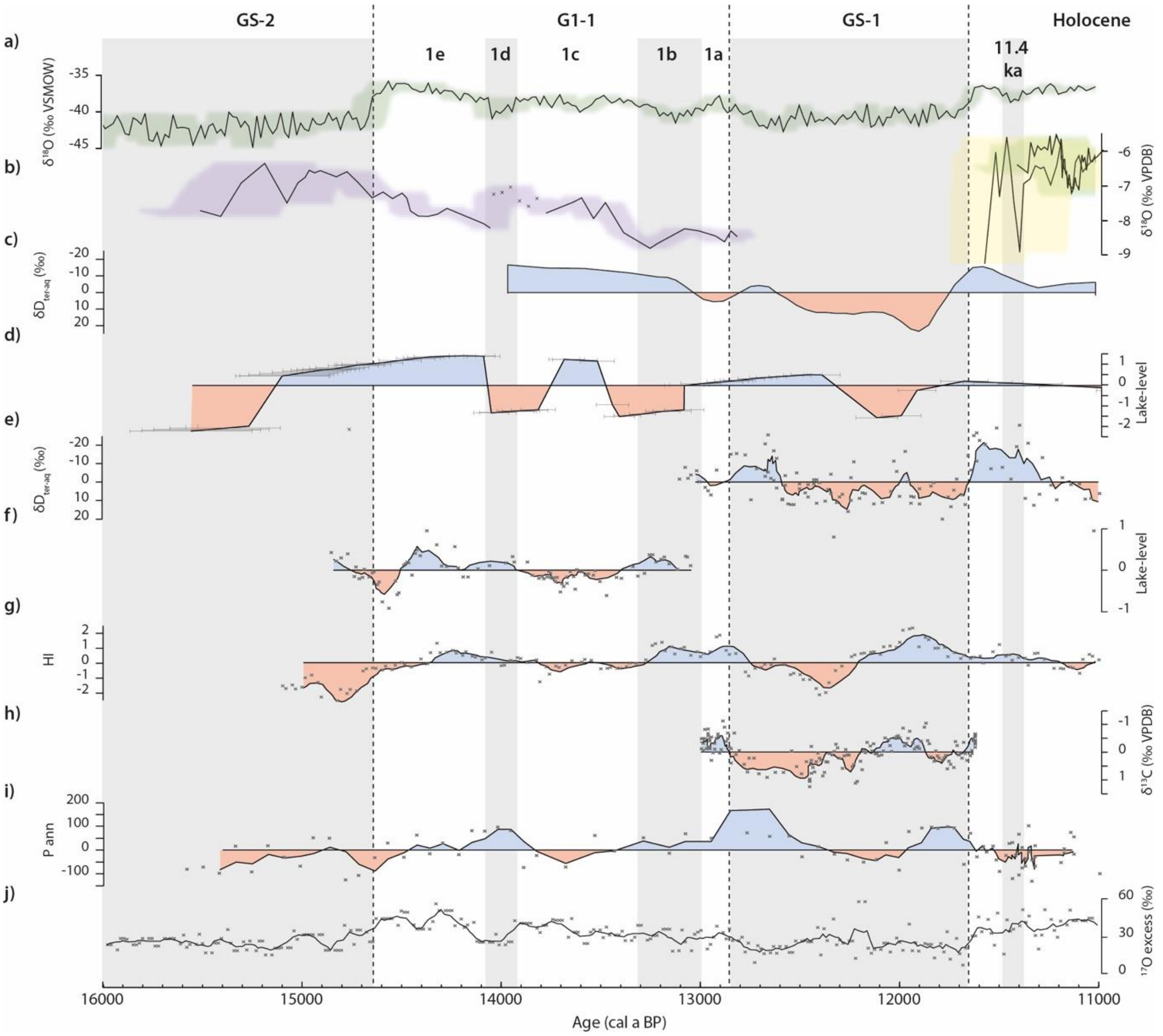


Figure 9. Comparisons of European hydroclimatic records. a) $\delta^{18}O$ from NGRIP (Rasmussen et al., 2006); b) $\delta^{18}O_c$ from the Wykeham basin (purple, this study) and Palaeolake Flixton (yellow and green, Blockley et al., 2018) in the VoP; c) $\delta D_{terr\text{-}aq}$ from Hässeldala Port, S. Sweden (Muschitiello et al., 2015); d) Relative lake-level reconstructions from the Wykeham basin (this study); e) $\delta D_{terr\text{-}aq}$ from Meerfelder Maar, Germany (Rach et al., 2014); f) Relative lake-level reconstructions from Lake Gerzensee, Switzerland (Magny, 2013); g) a hydrological index from a speleothem in Grotta Savi NE Italy (Belli et al., 2017); h) $\delta^{13}C$ isotopes from Seso Cave speleothems in NE Spain (Bartolome et al., 2015); i) reconstructed annual precipitation from Lake Navamuno, Central Spain (López-Sáez et al., 2020), and j) $^{17}O$ excess, a proxy for midlatitude moisture source conditions for Greenlandic precipitation (Landais et al., 2018). Hydrological records are presented as residuals from a linear smooth line (section 3.3; Figure 7) with positive residuals (blue) indicating humid signals, and negative residuals (red) indicating arid signals. The Meerfelder Maar, Lake Gerzensee, Grotta Savi, Navamuno and NGRIP $^{17}O$ excess records are displayed as 5 point moving averages with raw data presented as grey crosses. Grey bands represent cooling events in the Greenland ice cores (i.e. GS-2, GI-1d, GI-1b, GS-1, 11.4 ka event). The locations of these records relative to the VoP are shown in Figure 10.

During the centennial scale climatic oscillations of the Interstadial (~GI-1d and ~GI-1b), lower lake-levels persisted in the Wykeham basin, indicating low effective precipitation regimes recharging the VoP groundwater aquifer under arid hydroclimates. In Northern Europe, in regions between 50-60 ºN, low lake-levels (e.g. Bos et al., 2006) and high evapotranspiration signals (e.g. Rach et al., 2014; 2017; Muschitiello et al., 2015) have been recorded during these climatic oscillations, indicating transitions to more arid conditions in response to abrupt cooling events (section 5.5; Figure 9). Together, these trends show that cooler conditions during the Lateglacial Interstadial (~GI-1d and ~GI-1b), coincided with more arid hydroclimates across abrupt (sub-centennial) transitions in Northern Europe.

Central-Southern European records (between 50-40 ºN) show a different response, with higher relative lake-levels (e.g. Magny, 2013) and more humid hydroclimates (e.g. Belli et al., 2017; López-Sáez et al., 2020; Figure 9) persisting through the climatic oscillations of the Interstadial (~GI-1d and ~GI-1b). Hydrological trends through the Younger Dryas chronozone (~GI-1a to GS-1) show shifts to more arid hydroclimates across the European continent (Figure 9), but within this interval, there is additional complexity. The VoP and Northern European records are bi-partitioned into an early humid (high lake-level) phase, followed by a more arid (lower lake-level) phase (Magny and Ruffadi, 1995; Walker, 1995; Diefendorf et al., 2006; Bos et al., 2006). Further south in the Alps and the Iberian Peninsula, more humid conditions/higher lake-levels were initiated during the late Younger Dryas (< 12.5-12.15 ka BP; e.g. Bartolome et al., 2015; Rossi et al., 2018), prior to Northern Europe. Together these trends demonstrate that hydrological variations are more regionally dynamic than changes in temperature through the LGIT, and that hydrological responses to different cooling phases were manifested differently across the European continent, not necessarily occurring in phase with changes in temperature (Rach et al., 2014).

In the present day, hydroclimatic conditions in the British Isles and NW Europe are largely a function of the position of atmospheric circulation patterns across the North Atlantic Ocean. Interannual to centennial-scale variability in these circulation patterns are manifested through the North Atlantic Oscillation (NAO), but variability in the contemporary modes of the NAO are unlikely to account for the hydroclimatic bifurcations observed through the LGIT for two reasons: 1) model simulations have demonstrated that the pattern of atmospheric circulation varied significantly from contemporary modes, largely due to differences in the initial boundary conditions (e.g. the thickness and extent of Northern Hemispheric ice sheets, greenhouse gas concentrations, sea level pressure, sea-ice extent etc.; e.g. Pausata et al., 2011; Löfverström and Lora, 2017); 2) records of aeolian activity through the LGIT suggest that during cooling intervals, stationary circulation regimes dominated by strong and zonal westerly winds devoid of moisture persisted across the European continent (e.g. Isarin et al., 1998; Brauer et al., 2008; Costas et al., 2016), which is counter to the current interannual modes of the NAO. Therefore, it is likely that mechanisms other than NAO variability are required to explain the bifurcating hydroclimatic signals observed through the abrupt cooling events.

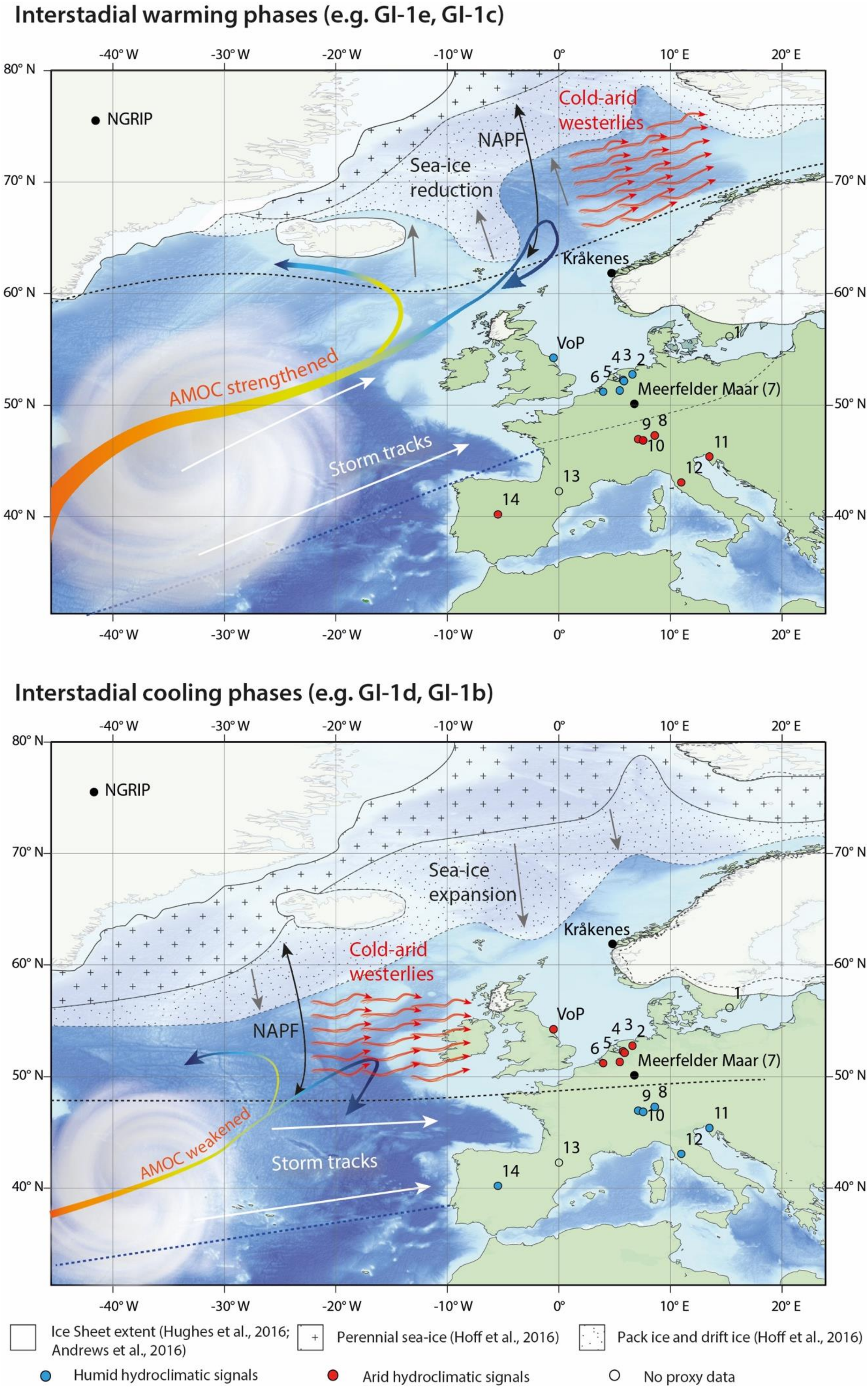
Interstadial warming phases (e.g. GI-1e, GI-1c)
NGRIP
NAPF
Cold-arid westerlies
Sea-ice reduction
Kråkenes
VoP
Meerfelder Maar (7)
AMOC strengthened
Storm tracks
1
2
3
4
5
6
8
9
10
11
12
13
14
Interstadial cooling phases (e.g. GI-1d, GI-1b)
NGRIP
Sea-ice expansion
Kråkenes
Cold-arid westerlies
NAPF
VoP
Meerfelder Maar (7)
AMOC weakened
Storm tracks
-40° W
-30° W
-20° W
-10° W
0°
10° E
20° E
80° N
70° N
60° N
50° N
40° N
Ice Sheet extent (Hughes et al., 2016; Andrews et al., 2016)
Perennial sea-ice (Hoff et al., 2016)
Pack ice and drift ice (Hoff et al., 2016)
Humid hydroclimatic signals
Arid hydroclimatic signals
No proxy data

Figure 10. Conceptual model illustrating the factors (latitude of sea-ice, NAPF, storm tracks and AMOC strength) responsible for bifurcating hydroclimatic signals during the cooling (GI-1d, GI-1b) and warming intervals (GI-1e, GI-1c) of the Lateglacial Interstadial (GI-1). Details of other hydrological records (1 to 14) displayed as either blue (humid), red (arid), or black (no proxy data) circles are listed in Appendix E. Hydrological proxy data from Hässeldala Port (1; Muschitiello et al., 2015; Wohlfarth et al., 2017), Meerfelder Maar (7; Rach et al., 2014), Lake Gerzensee (10; Magny, 2013), Grotta Savi (11; Belli et al., 2017), Grotta Seso (Bartolome et al., 2015), and Lake Navamuno (López-Sáez et al., 2020) are shown in Figure 9. The sites of Meerfelder Maar and Kråkenes, used as key locations to explain hydroclimatic variability during GS-1 (e.g. Bakke et al., 2009; Lane et al., 2013) are also shown. The extent of the Fennoscandian and British-Irish Ice sheet extents follow Hughes et al. (2016), Greenland and Iceland ice sheet extents follow Andrews et al. (2018), and estimations of sea-ice extent in the North Atlantic follows Hoff et al. (2016). The position of the NAPF, storm tracks, and cold westerly air masses follows the relative hydrological proxy signals from the records, and descriptions by Brauer et al. (2008); Naughton et al. (2019).

Climatic oscillations during the LGIT (GI-1d, GI-1b, GS-1) are most readily attributed to fluctuations in the Atlantic Meridional Overturning Circulation (AMOC) strength via freshwater hosing from the deglaciating Northern Hemispheric ice sheets, disrupting the transfer of latent heat to the continental margins (Broecker and Denton, 1989; Broecker et al*.,* 1990). Changes in regional hydrology associated with these events are attributed to the displacement of moisture bearing westerly winds across the European continent (e.g. Magny et al., 2007; Bakke et al., 2009), and should therefore most strongly affect the hydroclimates of western Europe.

Hydrological bifurcations between Northern and Southern Europe through the climatic oscillations of the LGIT occurred in association with changes in $^{17}$O-excess in the Greenland ice cores (Figure 9), interpreted as a proxy for the reorganization of climatic conditions and/or water cycle at latitudes south of Greenland (Guillevic et al., 2014; Landais et al., 2018). It is therefore assumed that hydroclimatic regimes in Europe were sensitive to perturbations in the mid-latitude water cycle, which would have been driven, at least in part, by shifts in the strength and latitude of the jet stream and the position of precipitation-bearing westerly winds across the continent (e.g. Bakke et al., 2009; Lane et al., 2013; Rach et al., 2014), which are themselves sensitive to the latitude of North Atlantic winter sea-ice cover (Isarin et al., 1998; Renssen and Isarin, 2001; Sadatzki et al., 2019; Figure 10).

The position of the North Atlantic Polar Front (NAPF), is a key constituent of hydroclimatic conditions in western Europe (Ruddiman and McIntyre, 1981). Collectively, the regional comparisons discussed above support that during the abrupt climatic events of the LGIT, winter sea-ice expansion in the North Atlantic initiated a southerly migration of the NAPF (e.g. Denton et al., 2005; Renssen et al., 2018; Muschitiello et al., 2019; Naughton et al., 2019), the focussing of stronger and more zonal westerly winds devoid of moisture across Northern Europe (Brauer et al., 2008), and the depression of moisture bearing subpolar cyclonic activity into Central and Southern Europe (e.g. Marchal et al., 2016; Pauly et al., 2018). This caused increased aridity between *ca* 50 to 60 ºN (e.g. Hoek and Bohncke, 2002; Bos et al., 2006) and increased humidity between *ca* 40 to 50 ºN (Magny, 2001; Belli et al., 2017). Regional hydrological bifurcations similar to those observed during the climatic oscillations of the Lateglacial Interstadial have been reconstructed during the Early Holocene (e.g. the 11.4 ka event and the 8.2 ka event; Magny et al., 2003; 2007), suggesting that this is a consistent response to abrupt cooling events during both glacial and interglacial climatic regimes across the European continent.

Changes in hydroclimatic signals through GS-1 (including the Younger Dryas in Europe) are more complex than those in GI-1d and GI-1b, and have also been attributed to the position of the NAPF across the European continent (e.g. Brauer et al., 2008; Bakke et al., 2009; Lane et al., 2013; Rach et al., 2014; Naughton et al., 2019). The findings presented here broadly supports these interpretations (i.e. enhanced Northern European aridity associated with cooling; Figure 9), but also highlight that this model is too simplistic, and cannot explain the internal hydroclimatic structure and leads and lags associated in GS-1. This is most notable during the initial stages of GS-1 (i.e. *ca* 12.90 to 12.70 cal ka BP), where more humid conditions in Northern European records persist for *ca* 0.17 ka after the onset of GS-1, before switching to arid hydroclimatic signals at the start of the Younger Dryas at *ca* 12.68 cal ka BP (e.g. Rach et al., 2014; Muschitiello et al., 2015). Although not precisely chronologically constrained at Wykeham (section 5.5), a similar signal of relatively humid conditions persisting during the initial stages of GS-1 (WU-6) before an abrupt transition to a more arid signal (WU-7a) is also recorded. This indicates that the shifts to colder conditions during GS-1 did not immediately lead to more arid hydroclimates in Northern Europe. In contrast, during the Lateglacial Interstadial climatic events, cooling is associated with what appears to be an immediate change to increased aridity in Northern Europe, a change that is also detected within chronological uncertainties to temperature ($\delta^{18}O$) changes in the Greenland ice cores (Rasmussen et al., 2014).

One explanation for the lag in hydrological response during GS-1 is the time taken for the southerly displacement and stabilisation of the NAPF and sea-ice edge in the North Atlantic Ocean in response to reduced AMOC strength (Rach et al., 2014). It should also be noted that the hydrological lag in Europe to cooling at the start of GS-1 is longer than the entire duration of GI-1d in the Greenland ice cores (*ca* 0.12 ka), which suggests that the hydrological and environmental responses to the abrupt cooling episodes of the Lateglacial Interstadial (GI-1b and GI-1d) were more closely synchronised with regional cooling than at the onset of the GS-1/YD period. Whilst there may be some limitations to these comparisons on the basis of chronological resolution, it is clear that hydroclimatic changes associated with abrupt climatic changes in Europe were dynamic, and cannot be assumed to occur concurrently with either: a) $\delta^{18}O$ changes in the Greenland ice cores (e.g. Bakke et al., 2009; Rach et al., 2014; Muschitiello et al., 2015); or b) hydrological changes occurring across the rest of the European continent. Further high-resolution records, coupled with robust chronologies are therefore required, particularly during intervals of abrupt changes in temperature, to further investigate the spatiotemporal differences and more precisely constrain the hydroclimatic leads and lags associated with these events.

## 7. Conclusions

The palaeolake basin at Wykeham Quarry provides the only currently available high-resolution, chronologically constrained account of hydroclimatic changes, coupled with changes in local environmental conditions, occurring in the British Isles through the LGIT. Several climatic oscillations are identified, which affected catchment vegetation cover and lake-levels, demonstrating a direct link between cooling intervals and phases of enhanced aridity in NE England. During cooling intervals (~GI-1d, ~GI-1b, ~GS-1), the local environment was dominated open ground perennial taxa, which were replaced by shrub-rich flora (e.g. *Empetrum nigrum,* and *Juniperus communis*) during the warmer episodes (~GI-1e, ~GI-1c). Based upon comparisons with the Greenland ice-core event stratigraphy, it is clear that hydrological shifts in the VoP were, in some instances asynchronous with temperature changes in Greenland. Comparisons to hydrological records elsewhere in Europe show a latitudinal bifurcation, with Northern European records becoming more arid, and southern records becoming more humid in response to climatic events during the Lateglacial Interstadial (GI-1d and GI-1b). Hydroclimatic signals in GS-1 are more complex, with Northern Europe initially becoming more humid before a secondary phase of enhanced aridity. In Central and Southern European records, the opposite trend is seen, with enhanced aridity transitioning to more humid hydroclimates. Shifting positions of the polar front across the North Atlantic seaboard in response to AMOC strength, and the position of the sea-ice margin, is thought to explain this phenomenon. The additional complexity within GS-1 however is not readily explained using these criteria, and further records are required to test these hypotheses. While the evidence for dynamic shifts in hydroclimate exist across Europe, these interpretations are based on a limited number of locations and a variety of methods. Additional high-resolution hydroclimatic records coupled with robust chronologies are required in order to further investigate hydroclimatic leads and lags, and patterns of spatiotemporal differences associated with intervals of abrupt climatic change through the LGIT.

## Acknowledgements

This work was undertaken as part of PCL's PhD research, funded by Hanson Aggregates. PCL gratefully acknowledges Robert Pigg for access to the land and to Stuart Laws and Tim Harvey from Hanson Aggregates for access, advice, and assistance whilst working at Wykeham Quarry. The authors also extend thanks to Ashley Abrook, Rhys Timms, and the MSc Quaternary Science cohort of 2014-2015 for assistance in the field, to David Lowry for the use of the stable isotope laboratory in the Department of Earth Sciences at Royal

Holloway, and to Jenni Sherriff for valuable discussions on the interpretation of the $\delta^{18}O$ and $\delta^{13}C$ results. The authors also wish to thank two anonymous reviewers who provided valuable constructive comments and recommendations on the original submitted draft which have significantly improved the quality of the manuscript.

## References

Abrook, A., 2017. Vegetation changes at Palaeolake Flixton during the Late-glacial and Early Holocene periods. In: Lincoln, P.C. Eddey, L.J., Matthews, I.P., Palmer, A.P. and Bateman, M.D. (eds.). 2017. The Quaternary of the Vale of Pickering: Field Guide. Quaternary Research Association, London.

Alonso-Zarza, A.M., 2003. Palaeoenvironmental significance of palustrine carbonates and calcretes in the geological record. *Earth-Science Reviews*, *60*(3-4), pp.261-298.

Andrews, J.T., Cabedo-Sanz, P., Jennings, A.E., Olafsdottir, S., Belt, S.T. and Geirsdóttir, Á., 2018. Sea ice, ice-rafting, and ocean climate across Denmark Strait during rapid deglaciation (~ 16–12 cal ka BP) of the Iceland and East Greenland shelves. *Journal of Quaternary Science*, *33*(1), pp.112-130.

Ashley, G.M., 1975. Rhythmic sedimentation in glacial lake Hitchcock, Massachusetts, Connecticut. In: Jopling, A.V., McDonald, B.C. (Eds.). Glaciofluvial and Glaciolacustrine Sedimentation. Society of Economic Palaeontologists and Mineralogists, Special Publication No. 23, pp. 304-320.

Atkinson, T. C., Briffa, K. R., and Coope, G. R. 1987. Seasonal temperatures in Britain during the past 22,000 years, reconstructed using beetle remains. *Nature*, *325*, 587-592.

Bakke, J., Lie, Ø., Heegaard, E., Dokken, T., Haug, G.H., Birks, H.H., Dulski, P. and Nilsen, T., 2009. Rapid oceanic and atmospheric changes during the Younger Dryas cold period. *Nature Geoscience*, *2*(3), pp.202-205.

Bartolomé, M., Moreno, A., Sancho, C., Stoll, H.M., Cacho, I., Spötl, C., Belmonte, Á., Edwards, R.L., Cheng, H. and Hellstrom, J.C., 2015. Hydrological change in Southern Europe responding to increasing North Atlantic overturning during Greenland Stadial 1. *Proceedings of the National Academy of Sciences*, *112*(21), pp.6568-6572.

Batchelor, C.R. 2009. Northern Extension and Southern Extensions, Wykeham Quarry: Geoarchaeological Deposit Models, Interim Report. Quaternary Scientific Unpublished Report

Battarbee, R.W., 2000. Palaeolimnological approaches to climate change, with special regard to the biological record. *Quaternary Science Reviews*, *19*(1-5), pp.107-124.

Bearcock, J.M.; Smedley, P.L.; Milne, C.J. 2016. *Baseline groundwater chemistry: the Corallian of the Vale of Pickering, Yorkshire.* Nottingham, UK, British Geological Survey, 70pp. (OR/15/048)

Belli, R., Borsato, A., Frisia, S., Drysdale, R., Maas, R. and Greig, A., 2017. Investigating the hydrological significance of stalagmite geochemistry (Mg, Sr) using Sr isotope and particulate element records across the Late Glacial-to-Holocene transition. *Geochimica et Cosmochimica Acta*, *199*, pp.247-263.

Bennike, O., 1998. Fossil egg sacs of Diaptomus (Crustaceae: Copepoda) in Late Quaternary lake sediments. *Journal of Paleolimnology*, *19*(1), pp.77-79.

Berggren, G., 1964. Atlas of Seeds. Part 2. Cyperaceae. Swedish Natural Science Research

Birks, H. H., 1980. Plant macrofossils in Quaternary lake sediments. Archiv fur Hydrobiologie Beiheft, 15: 1–60.

Birks, H.H., 2002. Plant macrofossils. In *Tracking environmental change using lake sediments* (pp. 49-74). Springer Netherlands.

Birks, H.H. and Birks, H.J.B., 2014. To what extent did changes in July temperature influence Lateglacial vegetation patterns in NW Europe? Quaternary Science Reviews, 106, pp.262-277.

Birks, H.H. and Mathewes, R.W., 1978. Studies in the vegetational history of Scotland. *New Phytologist*, *80*(2), pp.455-484.

Blockley, S.P., Lowe, J.J., Walker, M.J., Asioli, A., Trincardi, F., Coope, G.R. and Donahue, R.E., 2004. Bayesian analysis of radiocarbon chronologies: examples from the European Late-glacial. *Journal of Quaternary Science*, *19*(2), pp.159-175.

Blockley, S., Candy, I., Matthews, I., Langdon, P., Langdon, C., Palmer, A., Lincoln, P.C., Abrook, A., Taylor, B., Conneller, C. and Bayliss, A., 2018. The resilience of postglacial hunter-gatherers to abrupt climate change. *Nature ecology & evolution*, *2*(5), p.810.

Bos, J.A., Bohncke, S.J. and Janssen, C.R., 2006. Lake-level fluctuations and small-scale vegetation patterns during the late glacial in The Netherlands. *Journal of Paleolimnology*, *35*(2), pp.211-238.

Boston, C.M., Lukas, S. and Carr, S.J., 2015. A Younger Dryas plateau icefield in the Monadhliath, Scotland, and implications for regional palaeoclimate. *Quaternary Science Reviews*, 108, pp.139-162.

Brauer, A., Haug, G.H., Dulski, P., Sigman, D.M. and Negendank, J.F., 2008. An abrupt wind shift in western Europe at the onset of the Younger Dryas cold period. *Nature Geoscience*, *1*(8), pp.520-523.

Brock, F., Higham, T., Ditchfield, P. and Bronk Ramsey, C., 2010. Current pretreatment methods for AMS radiocarbon dating at the Oxford Radiocarbon Accelerator Unit (ORAU). *Radiocarbon*, *52*(1), pp.103-12.

Broecker, W.S. and Denton, G.H., 1989. The role of ocean-atmosphere reorganizations in glacial cycles. *Geochimica et Cosmochimica Acta*, *53*(10), pp.2465-2501.

Broecker, W.S., Bond, G., Klas, M., Bonani, G. and Wolfli, W., 1990. A salt oscillator in the glacial Atlantic? 1. The concept. *Paleoceanography*, *5*(4), pp.469-477.

Bronk Ramsey, C. (2008). Deposition models for chronological records. *Quaternary Science Reviews, 27*(1-2), 42-60.

Bronk Ramsey, C. (2009). Dealing with outliers and offsets in radiocarbon dating. *Radiocarbon, 51*(3), 1023-1045.

Bronk Ramsey, C., and Lee, S. (2013). Recent and Planned Developments of the Program OxCal. *Radiocarbon, 55*(2-3), 720-730.

Brooks, S.J. and Birks, H.J.B., 2000. Chironomid-inferred Late-glacial air temperatures at Whitrig Bog, Southeast Scotland. *Journal of Quaternary Science*, *15*(8), pp.759-764.

Brooks, S.J., Matthews, I.P., Birks, H.H. and Birks, H.J.B., 2012. High resolution Lateglacial and early-Holocene summer air temperature records from Scotland inferred from chironomid assemblages. *Quaternary Science Reviews*, *41*, pp.67-82.

Brown, T., Bradley, C., Grapes, T. and Boomer, I., 2011. Hydrological assessment of Star Carr and the Hertford catchment, Yorkshire, UK. *Journal of Wetland Archaeology*, *11*(1), pp.36-55.

Buizert, C., Gkinis, V., Severinghaus, J.P., He, F., Lecavalier, B.S., Kindler, P., Leuenberger, M., Carlson, A.E., Vinther, B., Masson-Delmotte, V. and White, J.W., 2014. Greenland temperature response to climate forcing during the last deglaciation. *Science*, *345*(6201), pp.1177-1180.

Bullock, P., Fedoroff, N., Jongerius, A., Stoops, G., Tursina, T. 1985. *Handbook for soil thin section description*, Waine Research, Chicago.

Candy, I., Farry, A., Darvill, C. M., Palmer, A., Blockley, S. P. E., Matthews, I. P., MacLeod, A., Deeprose, L., Farley, N., Kearney, R., Conneller, C., Taylor, B., and Milner, N., 2015. The evolution of Palaeolake Flixton and the environmental context of Star Carr: an oxygen and carbon isotopic record of environmental change for the early Holocene. *Proceedings of the Geologists' Association*, *126*(1), 60-71.

Candy, I., Abrook, A., Elliot, F., Lincoln, P., Matthews, I.P. and Palmer, A., 2016. Oxygen isotopic evidence for high-magnitude, abrupt climatic events during the Lateglacial Interstadial in north-west Europe: analysis of a lacustrine sequence from the site of Tirinie, Scottish Highlands. *Journal of Quaternary Science*, *31*(6), pp.607-621.

Candy, I., Palmer, A.P., Blockley, S.P.E., Matthews, I.P., MacLeod, A., Farley, N., Farry, A., Kearney, R., Abrook, A., Darvill., C. $\delta^{13}C$ and $\delta^{18}O$ analysis of lacustrince marls from Palaeolake Flixton. In: Lincoln, P.C. Eddey, L.J., Matthews, I.P., Palmer, A.P. and Bateman, M.D. (eds.). 2017. The Quaternary of the Vale of Pickering: Field Guide. Quaternary Research Association, London.

Cappers, R.T., René, T.J., Becker, R.M. and Jans, J.E., 2006. *Digital seed atlas of the Netherlands. Groningen Archaeological Studies, Volume 4*. Barkhuis Publishing and Groningen University Library, Groningen, 502pp. (in Dutch). Clark et al., 2001

Carey, M.A. and Chadha, D., 1998. Modelling the hydraulic relationship between the River Derwent and the Corallian Limestone aquifer. *Quarterly Journal of Engineering Geology and Hydrogeology*, *31*(1), pp.63-72.

Cerling T.E., and Quade J. 1993. Stable carbon and oxygen isotopes in soil carbonates. In: *Climate Change in Continental Isotopic Records*, Swart P.K., Lohmann K.C., Mckenzie J., Savin S. (eds). American Geophysical Union, Washington, DC; 217–231.

Chandler, B.M., Boston, C.M. and Lukas, S., 2019. A spatially-restricted Younger Dryas plateau icefield in the Gaick, Scotland: Reconstruction and palaeoclimatic implications. *Quaternary Science Reviews*, 211, pp.107-135.

Clark, P.U., Pisias, N.G., Stocker, T.F. and Weaver, A.J., 2002. The role of the thermohaline circulation in abrupt climate change. *Nature*, *415*(6874), pp.863-869.

Cohen, A.S., 2003. *Paleolimnology: the history and evolution of lake systems*. Oxford University Press.

Costas, S., Naughton, F., Goble, R. and Renssen, H., 2016. Windiness spells in SW Europe since the last glacial maximum. *Earth and Planetary Science Letters*, *436*, pp.82-92.

Darling, W. G. 2004. Hydrological factors in the interpretation of stable isotopic proxy data present and past: a European perspective. *Quaternary Science Reviews*, 23 (7), 743-770.

Day, P., 1996. Devensian Late-glacial and early Flandrian environmental history of the Vale of Pickering, Yorkshire, England*. Journal of Quaternary Science,* 11, 9-24.

Dean, W.E., 1974. Determination of carbonate and organic matter in calcareous sediments and sedimentary rocks by loss on ignition: comparison with other methods. *Journal of Sedimentary Research*, *44*(1).

Denton, G.H., Alley, R.B., Comer, G.C. and Broecker, W.S., 2005. The role of seasonality in abrupt climate change. *Quaternary Science Reviews*, *24*(10), pp.1159-1182.

Diefendorf, A.F., Patterson, W.P., Mullins, H.T., Tibert, N. and Martini, A., 2006. Evidence for high-frequency late Glacial to mid-Holocene (16,800 to 5500 cal yr BP) climate variability from oxygen isotope values of Lough Inchiquin, Ireland. *Quaternary Research*, *65*(1), pp.78-86.

Dieffenbacher-Krall, A. and Halteman, W., 2000. The relationship of modern plant remains to water depth in alkaline lakes in New England, USAe. *Journal of Paleolimnology*, *24*(2), pp.213-229.

Evans, D.J., Bateman, M.D., Roberts, D.H., Medialdea, A., Hayes, L., Duller, G.A., Fabel, D. and Clark, C.D., 2017. Glacial Lake Pickering: stratigraphy and chronology of a proglacial lake dammed by the North Sea Lobe of the British–Irish Ice Sheet. *Journal of Quaternary Science*. *32* (2). 295-310

Gale, S. J. and Hoare, P. G. 1991 *Quaternary sediments: petrographic methods for the study of unlithified rocks*, Belhaven, London.

Genty, D., Blamart, D., Ghaleb, B., Plagnes, V., Causse, C., Bakalowicz, M., Zouari, K., Chkir, N., Hellstrom, J., Wainer, K. and Bourges, F., 2006. Timing and dynamics of the last deglaciation from European and North African δ13C stalagmite profiles—comparison with Chinese and South Hemisphere stalagmites. *Quaternary Science Reviews*, *25*(17-18), pp.2118-2142.

Guillevic, M., Bazin, L., Landais, A., Stowasser, C., Masson-Delmotte, V., Blunier, T., Eynaud, F., Falourd, S., Michel, E., Minster, B. and Popp, T., 2014. Evidence for a three-phase sequence during Heinrich Stadial 4 using a multiproxy approach based on Greenland ice core records. *Climate of the Past*, *10*(6), pp.2115-2133.

Hammarlund, D., Björck, S., Buchardt, B., Israelson, C. and Thomsen C.T., 2003. Rapid hydrological changes during the Holocene revealed by stable isotope records of lacustrine carbonates from Lake Igelsjön, southern Sweden. *Quaternary Science Reviews*, 22, 353–370.

Hannon, G.E. and Gaillard, M.J., 1997. The plant-macrofossil record of past lake-level changes. *Journal of Paleolimnology*, *18*(1), pp.15-28.

Harrison, S.P. and Digerfeldt, G., 1993. European lakes as palaeohydrological and palaeoclimatic indicators. *Quaternary Science Reviews*, *12*(4), pp.233-248.

Hays P.D. and Grossman E.L. 1991. Oxygen isotopes in meteoric calcite cements as indicators of continental paleoclimate. *Geology* 19: 441–444.

Heiri, O., Cremer, H., Engels, S., Hoek, W.Z., Peeters, W. and Lotter, A.F., 2007. Lateglacial summer temperatures in the Northwest European lowlands: a chironomid record from Hijkermeer, the Netherlands. *Quaternary Science Reviews*, 26(19), pp.2420-2437.

Heiri, O., Brooks, S.J., Renssen, H., Bedford, A., Hazekamp, M., Ilyashuk, B., Jeffers, E.S., Lang, B., Kirilova, E., Kuiper, S. and Millet, L., 2014. Validation of climate model-inferred regional temperature change for late-glacial Europe. *Nature communications*, *5*, p.4914.

Hoek, W.Z. and Bohncke, S.J.P., 2002. Climatic and environmental events over the Last Termination, as recorded in The Netherlands: a review. *Netherlands Journal of Geosciences/Geologie en Mijnbouw*, *81*(1).

Hoff, U., Rasmussen, T.L., Stein, R., Ezat, M.M. and Fahl, K., 2016. Sea ice and millennial-scale climate variability in the Nordic seas 90 kyr ago to present. *Nature communications*, *7*, p.12247.

Hughes, A.L., Gyllencreutz, R., Lohne, Ø.S., Mangerud, J. and Svendsen, J.I., 2016. The last Eurasian ice sheets–a chronological database and time-slice reconstruction, DATED-1. *Boreas*, *45*(1), pp.1-45.

Isarin, R.F., Renssen, H. and Vandenberghe, J., 1998. The impact of the North Atlantic Ocean on the Younger Dryas climate in northwestern and central Europe. *Journal of Quaternary Science*, *13*(5), pp.447-453.

Kendall, P.F., 1902. A system of glacier-lakes in the Cleveland Hills. *Quarterly Journal of the Geological Society*, *58*(1-4), pp.471-571.

Kim S. and O'Neil J.R.. 1997. Equilibrium and nonequilibrium oxygen isotope effects in synthetic carbonates. *Geochimica et Cosmochimica Acta,* 61: 3461–3475.

Landais, A., Capron, E., Masson-Delmotte, V., Toucanne, S., Rhodes, R.H., Popp, T., Vinther, B., Minster, B. and Prié, F., 2018. Ice core evidence for decoupling between midlatitude atmospheric water cycle and Greenland temperature during the last deglaciation. *Climate of the Past*, *14*(10), pp.1405-1415.

Lane, C.S., Brauer, A., Blockley, S.P. and Dulski, P., 2013. Volcanic ash reveals time-transgressive abrupt climate change during the Younger Dryas. *Geology*, *41*(12), pp.1251-1254.

Leng, M. J., and Marshall, J. D. 2004. Palaeoclimate interpretation of stable isotope data from lake sediment archives. *Quaternary Science Reviews*, 23 (7), 811-831.

Lincoln, P.C. Eddey, L.J., Matthews, I.P., Palmer, A.P. and Bateman, M.D. (eds.). 2017. The Quaternary of the Vale of Pickering: Field Guide. Quaternary Research Association, London.

López-Sáez, J.A., Carrasco, R.M., Turu, V., Ruiz-Zapata, B., Gil-García, M.J., Luelmo-Lautenschlaeger, R., Pérez-Díaz, S., Alba-Sánchez, F., Abel-Schaad, D., Ros, X. and Pedraza, J., 2020. Late Glacial-early holocene vegetation and environmental changes in the western Iberian Central System inferred from a key site: The Navamuño record, Béjar range (Spain). *Quaternary Science Reviews*, *230*, p.106-167.

Lotter, A.F., Heiri, O., Brooks, S., van Leeuwen, J.F., Eicher, U. and Ammann, B., 2012. Rapid summer temperature changes during Termination 1a: high-resolution multi-proxy climate reconstructions from Gerzensee (Switzerland). *Quaternary Science Reviews*, 36, pp.103-113.

Löfverström, M. and Lora, J.M., 2017. Abrupt regime shifts in the North Atlantic atmospheric circulation over the last deglaciation. *Geophysical Research Letters*, *44*(15), pp.8047-8055.

Lowe, J.J., Coope, G.R., Sheldrick, C., Harkness, D.D. and Walker, M.J.C., 1995. Direct comparison of UK temperatures and Greenland snow accumulation rates, 15000—12000 yr ago. *Journal of Quaternary Science*, *10*(2), pp.175-180.

Lowe, J.J., Matthews, I.P., Mayfield, R., Lincoln, P.C., Palmer, A.P, Staff, R.A. and Timms, R.G.O., 2019. On the timing of retreat of the Loch Lomond ('Younger Dryas') Readvance icefield in the SW Scottish Highlands and its wider significance. *Quaternary Science Reviews*, 219, pp.171-186.

Magny, M. and Ruffadi, P., 1995. Younger Dryas and early Holocene lake-level fluctuations in the Jura mountains, France. *Boreas*, *24*(2), pp.155-172.

Magny, M., Bégeot, C., Guiot, J. and Peyron, O., 2003. Contrasting patterns of hydrological changes in Europe in response to Holocene climate cooling phases. *Quaternary Science Reviews*, 22(15-17), pp.1589-1596.

Magny, M., Vannière, B., De Beaulieu, J.L., Bégeot, C., Heiri, O., Millet, L., Peyron, O. and Walter-Simonnet, A.V., 2007. Early-Holocene climatic oscillations recorded by lake-level fluctuations in west-central Europe and in central Italy. *Quaternary Science Reviews*, *26*(15), pp.1951-1964.

Magny, M., 2013. Climatic and environmental changes reflected by lake-level fluctuations at Gerzensee from 14,850 to 13,050 yrBP. *Palaeogeography, Palaeoclimatology, Palaeoecology*, *391*, pp.33-39.

Mangerud, J., Aarseth, I., Hughes, A.L., Lohne, Ø.S., Skår, K., Sønstegaard, E. and Svendsen, J.I., 2016. A major re-growth of the Scandinavian Ice Sheet in western Norway during Allerød-Younger Dryas. *Quaternary Science Reviews*, 132, pp.175-205.

Mangerud, J., Briner, J.P., Goslar, T. and Svendsen, J.I., 2017. The Bølling-age Blomvåg Beds, western Norway: implications for the Older Dryas glacial re-advance and the age of the deglaciation. *Boreas*, *46*(2), pp.162-184.

Marchal, O., Waelbroeck, C. and Colin de Verdière, A., 2016. On the movements of the North Atlantic subpolar front in the preinstrumental past. *Journal of Climate*, *29*(4), pp.1545-1571

Marshall, J. D., Jones, R. T., Crowley, S. F., Oldfield, F., Nash, S., and Bedford, A. 2002. A high resolution late-glacial isotopic record from Hawes Water, northwest England: Climatic oscillations: Calibration and comparison of palaeotemperature proxies. *Palaeogeography, Palaeoclimatology, Palaeoecology*, *185*(1), 25-40.

Marshall, J. D., Lang, B., Crowley, S. F., Weedon, G. P., van Calsteren, P., Fisher, E. H., Holme, R., Holmes, J.A., Jones, R.T., Bedford, A. and Brooks, S. J. 2007. Terrestrial impact of abrupt changes in the North Atlantic thermohaline circulation: Early Holocene, UK. *Geology*,*35*(7), 639-642.

Matthews, I.P., Birks, H.H., Bourne, A.J., Brooks, S.J., Lowe, J.J., MacLeod, A. and Pyne-O'Donnell, S.D.F., 2011. New age estimates and climatostratigraphic correlations for the Borrobol and Penifiler Tephras: evidence from Abernethy Forest, Scotland. *Journal of Quaternary Science*, *26*(3), pp.247-252.

Matthews, I.P., Abrook, A., Lincoln, P.C. and Palmer, A.P. The Last Glacial Interglacial Transition (16-8 ka BP) in North East England. In: Lincoln, P.C. Eddey, L.J., Matthews, I.P., Palmer, A.P. and Bateman, M.D. (eds.). 2017. The Quaternary of the Vale of Pickering: Field Guide. Quaternary Research Association, London.

Mauquoy D, van Geel B. 2007. Mire and peat macros. In Encyclopedia of Quaternary Science, Vol. 3, Elias SA (ed.). Elsevier: Amsterdam; 2315–2336.

McConnaughey, T., 1991. Calcification in Chara corallina: $CO_2$ hydroxylation generates protons for bicarbonate assimilation. *Limnology and Oceanography*, *36*(4), pp.619-628.

Mellars, P., and Dark, P., 1998. Star Carr in context: new archaeological and palaeoecolgical investigations at the early Mesolithic site of Star Carr, North Yorkshire. Cambridge: McDonald Institute.

Milner, N., Conneller, C. and Taylor, B., 2018. *Star Carr, Volume 1: a persistent place in a changing world*. White Rose University Press.

Moreno, A., Svensson, A., Brooks, S.J., Connor, S., Engels, S., Fletcher, W., Genty, D., Heiri, O., Labuhn, I., Perşoiu, A. and Peyron, O., 2014. A compilation of Western European terrestrial records 60–8 ka BP: towards an understanding of latitudinal climatic gradients. *Quaternary Science Reviews*, *106*, pp.167-185.

Mortensen, M. F., Birks, H. H., Christensen, C., Holm, J., Noe-Nygaard, N., Odgaard, B. V., Olsen, J. and Rasmussen, K. L. 2011. Lateglacial vegetation development in Denmark–new evidence based on macrofossils and pollen from Slotseng, a small-scale site in southern Jutland. *Quaternary Science Reviews*, *30*(19), 2534-2550.

Murphy, D.H. and Wilkinson, B.H., 1980. Carbonate deposition and facies distribution in a central Michigan marl lake. *Sedimentology*, *27*(2), pp.123-135.

Muschitiello, F., Pausata, F.S., Watson, J.E., Smittenberg, R.H., Salih, A.A., Brooks, S.J., Whitehouse, N.J., Karlatou-Charalampopoulou, A. and Wohlfarth, B., 2015. Fennoscandian freshwater control on Greenland hydroclimate shifts at the onset of the Younger Dryas. *Nature communications*, *6*, 8939.

Muschitiello, F., D'Andrea, W.J., Schmittner, A., Heaton, T.J., Balascio, N.L., DeRoberts, N., Caffee, M.W., Woodruff, T.E., Welten, K.C., Skinner, L.C. and Simon, M.H., 2019. Deep-water circulation changes lead North Atlantic climate during deglaciation. *Nature communications*, *10*(1), p.1272.

Naughton, F., Costas, S., Gomes, S.D., Desprat, S., Rodrigues, T., Goñi, M.S., Renssen, H., Trigo, R., Bronk-Ramsey, C., Oliveira, D. and Salgueiro, E., 2019. Coupled ocean and atmospheric changes during Greenland stadial 1 in southwestern Europe. *Quaternary Science Reviews*, 212, pp.108-120.

Palmer, A. P., Lee, J.A., Kemp, R.A., Carr, S.J. 2008. *Revised laboratory procedures for the preparation of thin sections from unconsolidated material*. Unpublished Internal Report, Royal Holloway, University of London.

Palmer, A.P., Matthews, I.P., Candy, I., Blockley, S.P.E., MacLeod, A., Darvill, C.M., Milner, N., Conneller, C. and Taylor, B., 2015. The evolution of Palaeolake Flixton and the environmental context of Star Carr, NE. Yorkshire: stratigraphy and sedimentology of the Last Glacial-Interglacial Transition (LGIT) lacustrine sequences. *Proceedings of the Geologists' Association*, *126*(1), pp.50-59.

Pauly, M., Helle, G., Miramont, C., Büntgen, U., Treydte, K., Reinig, F., Guibal, F., Sivan, O., Heinrich, I., Riedel, F. and Kromer, B., 2018. Subfossil trees suggest enhanced Mediterranean hydroclimate variability at the onset of the Younger Dryas. *Scientific reports*, 8(1), pp.1-8.

Pausata, F.S.R., Li, C., Wettstein, J.J., Kageyama, M., Nisancioglu, K.H., 2011. The key role of topography in altering North Atlantic atmospheric circulation during the last glacial period. *Climate of the Past*, 7 (4), 1089–1101. doi: 10.5194/cp-7-1089-2011.

Pentecost, A., 2009. The marl lakes of the British Isles. *Freshwater Reviews*, 2(2), pp.167-198.

Rach, O., Brauer, A., Wilkes, H. and Sachse, D., 2014. Delayed hydrological response to Greenland cooling at the onset of the Younger Dryas in western Europe. *Nature Geoscience*, *7*(2), pp.109-112.

Rach, O., Kahmen, A., Brauer, A. and Sachse, D., 2017. A dual-biomarker approach for quantification of changes in relative humidity from sedimentary lipid D∕H ratios. *Climate of the Past*, *13*(7), pp.741-757.

Rahmstorf, S., Feulner, G., Mann, M.E., Robinson, A., Rutherford, S. and Schaffernicht, E.J., 2015. Exceptional twentieth-century slowdown in Atlantic Ocean overturning circulation. *Nature climate change*, *5*(5), pp.475-480.

Rasmussen, S.O., Andersen, K.K., Svensson, A.M., Steffensen, J.P., Vinther, B.M., Clausen, H.B., Siggaard-Andersen, M.L., Johnsen, S.J., Larsen, L.B., Dahl-Jensen, D. and Bigler, M., 2006. A new Greenland ice core chronology for the last glacial termination. *Journal of Geophysical Research: Atmospheres*, *111*(D6).

Rasmussen, S.O., Bigler, M., Blockley, S.P., Blunier, T., Buchardt, S.L., Clausen, H.B., Cvijanovic, I., Dahl-Jensen, D., Johnsen, S.J., Fischer, H. and Gkinis, V., 2014. A stratigraphic framework for abrupt climatic changes during the Last Glacial period based on three synchronized Greenland ice-core records: refining and extending the INTIMATE event stratigraphy. *Quaternary Science Reviews*, *106*, pp.14-28.

Reimer, P.J., Bard, E., Bayliss, A., Beck, J.W., Blackwell, P.G., Ramsey, C.B., Buck, C.E., Cheng, H., Edwards, R.L., Friedrich, M. and Grootes, P.M., 2013. IntCal13 and Marine13 radiocarbon age calibration curves 0–50,000 years cal BP. *Radiocarbon*, *55*(4), pp.1869-1887.

Renssen, H. and Isarin, R.F., 2001. The two major warming phases of the last deglaciation at∼ 14.7 and∼ 11.5 ka cal BP in Europe: climate reconstructions and AGCM experiments. *Global and Planetary Change*, *30*(1), pp.117-153.

Renssen, H., Goosse, H., Roche, D.M. and Seppä, H., 2018. The global hydroclimate response during the Younger Dryas event. *Quaternary Science Reviews*, 193, pp.84-97.

Rossi, C., Bajo, P., Lozano, R.P. and Hellstrom, J., 2018. Younger Dryas to Early Holocene paleoclimate in Cantabria (N Spain): Constraints from speleothem Mg, annual fluorescence banding and stable isotope records. *Quaternary Science Reviews*, *192*, pp.71-85.

Rozanski, K., Araguas-Araguas, L. and Gonfiantini, R., 1992. Relation between long-term trends of oxygen-18 isotope composition of precipitation and climate. *Science*, *258*(5084), pp.981-985.

Rozanski, K, Araguas-Araguas, L. and Gonfiantini R. 1993. Isotopic patterns in modern global precipitation. In Climate Change in Continental Isotopic Records, Swart PK, Lohmann KC, McKenzie J, Savin S (eds). American Geophysical Union: Washington, DC; 1–36.

Ruddiman, W.F. and McIntyre, A., 1981. The North Atlantic Ocean during the last deglaciation. *Palaeogeography, Palaeoclimatology, Palaeoecology*, *35*, pp.145-214.

Sadatzki, H., Dokken, T.M., Berben, S.M., Muschitiello, F., Stein, R., Fahl, K., Menviel, L., Timmermann, A. and Jansen, E., 2019. Sea ice variability in the southern Norwegian Sea during glacial Dansgaard-Oeschger climate cycles. *Science advances*, *5*(3), p.eaau6174.

Samartin, S., Heiri, O., Lotter, A.F. and Tinner, W., 2012. Climate warming and vegetation response after Heinrich event 1 (16 700–16 000 cal yr BP) in Europe south of the Alps. *Climate of the Past*, *8*(6), pp.1913-1927.

Schillereff, D.N., Chiverrell, R.C., Macdonald, N. and Hooke, J.M., 2015. Flood stratigraphies in lake sediments: A review. *Earth-Science Reviews*, *135*, pp.17-37.

Shakun, J.D., Clark, P.U., He, F., Marcott, S.A., Mix, A.C., Liu, Z., Otto-Bliesner, B., Schmittner, A. and Bard, E., 2012. Global warming preceded by increasing carbon dioxide concentrations during the last deglaciation. *Nature*, 484(7392), p.49.

Smith, A.J.E. and Smith, R., 2004. *The moss flora of Britain and Ireland*. Cambridge University Press.

Soulié-Märsche, I. and Garcia, A., 2015. Gyrogonites and oospores, complementary viewpoints to improve the study of the charophytes (Charales). *Aquatic Botany*, 120, 7–17

Spence, D.H.N. and Chrystal, J., 1970. Photosynthesis and zonation of freshwater macrophytes. 1. Depth distribution and shade tolerance. *New phytologist*, *69*(1), 205-215.

Steffensen, J.P., Andersen, K.K., Bigler, M., Clausen, H.B., Dahl-Jensen, D., Fischer, H., Goto-Azuma, K., Hansson, M., Johnsen, S.J., Jouzel, J. and Masson-Delmotte, V., 2008. High-resolution Greenland ice core data show abrupt climate change happens in few years. *Science*, *321*(5889), pp.680-684.

Talbot, M.R., 1990. A review of the palaeohydrological interpretation of carbon and oxygen isotopic ratios in primary lacustrine carbonates. *Chemical Geology: Isotope Geoscience Section*, *80*(4), pp.261-279.

Taylor, B., 2011. Early Mesolithic activity in the wetlands of the Lake Flixton Basin. *Journal of Wetland Archaeology*, *11*(1), 63-84.

Treese, K.L. and Wilkinson, B.H., 1982. Peat-marl deposition in a Holocene paludal-lacustrine basin—Sucker Lake, Michigan. *Sedimentology*, *29*(3), 375-390.

Tweddle, J.C., 2001. Regional vegetational history. In: Bateman, M.D., Buckland, P.C., Frederick, C.D., Whitehouse, N.J. (Eds.), The Quaternary of East Yorkshire and North Lincolnshire Field Guide. Quaternary Research Association, London, pp. 35–46.

Turney, C.S., Coope, G.R., Harkness, D.D., Lowe, J.J. and Walker, M.J., 2000. Implications for the dating of Wisconsinan (Weichselian) Late-Glacial events of systematic radiocarbon age differences between terrestrial plant macrofossils from a site in SW Ireland. *Quaternary Research*, 53(1), pp.114-121.

Tye, G.J., Sherriff, J., Candy, I., Coxon, P., Palmer, A., McClymont, E.L. and Schreve, D.C., 2016. The $\delta^{18}O$ stratigraphy of the Hoxnian lacustrine sequence at Marks Tey, Essex, UK: implications for the climatic structure of MIS 11 in Britain. *Journal of Quaternary Science*, *31*(2), pp.75-92.

van Asch, N., Lutz, A. F., Duijkers, M. C., Heiri, O., Brooks, S. J., and Hoek, W. Z. 2012. Rapid climate change during the Weichselian Lateglacial in Ireland: Chironomid-inferred summer temperatures from Fiddaun, Co. Galway. *Palaeogeography, Palaeoclimatology, Palaeoecology*, *315*, 1-11.

Van Geel, B., Bohncke, S.J.P. and Dee, H., 1980. A palaeoecological study of an upper Late Glacial and Holocene sequence from "De Borchert", The Netherlands. *Review of Palaeobotany and Palynology*, *31*, pp.367-448.

Van Geel, B., Coope, G. R., and Van Der Hammen, T. 1989. Palaeoecology and stratigraphy of the Lateglacial type section at Usselo (The Netherlands). *Review of Palaeobotany and Palynology*, *60*(1), 25-129.

Vandenberghe, J., 2008. The fluvial cycle at cold–warm–cold transitions in lowland regions: a refinement of theory. *Geomorphology*, *98*(3-4), pp.275-284.

Vellinga, M. and Wood, R.A., 2002. Global climatic impacts of a collapse of the Atlantic thermohaline circulation. *Climatic change*, *54*(3), pp.251-267.

von Grafenstein, U., Erlenkeuser, H., Brauer, A., Jouzel, J. and Johnsen, S.J., 1999. A mid-European decadal isotope-climate record from 15,500 to 5000 years BP. *Science*, *284*(5420), 1654-1657.

Wagner-Cremer, F. and Lotter, A.F., 2011. Spring-season changes during the Late Pleniglacial and Bølling/Allerød interstadial. *Quaternary Science Reviews*, *30*(15-16), 1825-1828.

Walker, M.J.C., 1995. Climatic changes in Europe during the last glacial/interglacial transition. *Quaternary International*, *28*, pp.63-76.

Walker, M.J.C., Coope, G.R. and Lowe, J.J., 1993. The Devensian (Weichselian) Lateglacial palaeoenvironmental record from Gransmoor, East Yorkshire, England: A contribution to the 'North Atlantic seaboard programme'of IGCP-253, 'Termination of the Pleistocene'. *Quaternary Science Reviews*, *12*(8), 659-680.

Walker, M.J.C., Coope, G.R., Sheldrick, C., Turney, C.S.M., Lowe, J.J., Blockley, S.P.E. and Harkness, D.D., 2003. Devensian Lateglacial environmental changes in Britain: a multi-proxy environmental record from Llanilid, South Wales, UK. *Quaternary Science Reviews*, *22*(5), 475-520.

Watson, J.E., Brooks, S.J., Whitehouse, N.J., Reimer, P.J., Birks, H.J.B. and Turney, C., 2010. Chironomid-inferred late-glacial summer air temperatures from Lough Nadourcan, Co. Donegal, Ireland. *Journal of Quaternary Science*, *25*(8), 1200-1210.

Watson, E.V., 1981. *British Mosses and Liverworts: An Introductory Work*. Cambridge University Press.

Whittington, G., Edwards, K.J., Zanchetta, G., Keen, D.H., Bunting, M.J., Fallick, A.E. and Bryant, C.L., 2015. Lateglacial and early Holocene climates of the Atlantic margins of Europe: Stable isotope, mollusc and pollen records from Orkney, Scotland. *Quaternary Science Reviews*, *122*, pp.112-130.

Wohlfarth, B., Muschitiello, F., L. Greenwood, S., Andersson, A., Kylander, M., Smittenberg, R.H., Steinthorsdottir, M., Watson, J. and Whitehouse, N.J., 2017. Hässeldala–a key site for Last Termination climate events in northern Europe. *Boreas*, *46*(2), pp.143-161.

Wohlfarth, B., Luoto, T.P., Muschitiello, F., Väliranta, M., Björck, S., Davies, S.M., Kylander, M., Ljung, K., Reimer, P.J. and Smittenberg, R.H., 2018. Climate and environment in southwest Sweden 15.5–11.3 cal. ka BP. *Boreas*, *47*(3), pp.687-710.

Yu, Z. and Eicher, U., 1998. Abrupt climate oscillations during the last deglaciation in central North America. *Science*, *282*(5397), pp.2235-2238.

Zhao, Y., Sayer, C.D., Birks, H.H., Hughes, M. and Peglar, S.M., 2006. Spatial representation of aquatic vegetation by macrofossils and pollen in a small and shallow lake. *Journal of Paleolimnology*, *35*(2), pp.335-350.

I wish to confirm that there are no known conflicts of interest associated with this publication and there has been no financial support for this work that could have influenced its outcome. All co-authors have given their consent and have read and approved this manuscript.

Yours Sincerely
Paul Lincoln

**Author contributions:**

**Ian Matthews:** PhD supervisor; member of the field sampling team; co-responsible for the construction of the age model and the relative lake level reconstructions; contributed to the writing of the paper

**Adrian Palmer:** PhD supervisor; member of the field sampling team; contributed to the writing of the paper

**Simon Blockley:** PhD supervisor; member of the field sampling team

**Ian Candy:** conducted some of the initial stable isotopic analyses; co-authored the stable isotopic interpretations; contributed to the writing of the paper

**Richard Staff:** conducted the AMS radiocarbon dating, advised on calibration and interpretation of the radiocarbon dates; co-responsible for the construction of the age model; contributed to the writing of the paper

**Paul Lincoln:** led the research project; leader of the field sampling team; conducted and interpreted the macroscale and microscale sedimentology; macrofossil sampling and identification, bulk carbonate isotopic analyses, and assisted with the AMS radiocarbon sample preparation at the University of Oxford; co-responsible for the construction of the age model; lead author for the paper and the production of all tables and figures.